The Quantitative Analysis of Martian Images: Evidence of Life?

Richard A. Armstrong

Vision Sciences, Aston University, Birmingham, B4 7ET, UK.

Journal of Astrobiology, Vol 16, Published January 2025

Abstract

Large numbers of photographs of the Martian landscape, including surface details of rock, boulders, and regolith, have been obtained by the Viking landers and the Spirit, Opportunity, Curiosity, and Perseverance rovers. Some of these photographs may reveal signs of possible life either in the form of fossil-like features or of living organisms such as algae, fungi, and lichens. The information which can be obtained from such photographs, however, is often limited, difficult to interpret, and highly controversial. Quantitative methods may help to determine whether an observed feature is evidence of a biological origin or the result of an abiotic process. This article describes various methods of quantifying the abundance and morphology of visible surface features on Mars and the sampling methods by which these measures can be obtained. The problem of establishing a scale measure for a quantitative analysis is discussed , methods of determining spatial pattern, i.e., whether a feature is distributed at random, regularly, or is aggregated into clusters, and the degree of spatial association between features are described. Quantitative morphological analysis is also described which may help to identify structures of biological interest by comparing them with feasible terrestrial analogues. The quantitative methods are illustrated with reference to the analysis of a number of 'life-like' Martian features including the dense populations of spherules photographed by Opportunity at *Meridiani Planum*, the lozenge-shaped 'rice-grains' photographed by Curiosity at Gale Crater, and the pitted rocks photographed by several rovers. The limitations of the various methods and future developments are also discussed.

Key Words: Quantitative analysis; Mars; 'Curiosity'; 'Opportunity'; 'Perseverance'; 'Viking'; Sampling methods; Dispersion; Spatial association

1. Introduction

Large numbers of photographs have been uploaded from the surface of Mars by the Viking landers and the Spirit, Opportunity, Curiosity, and Perseverance rovers. Hence, to date, over 650 000 photographs have been uploaded from Curiosity alone and include panoramic views of the landscape and more detailed images of pebbles, rocks, boulders, and regolith using the 'Mars Hand Lens Imager' (MAHLI) or Sherlock-Watson (S-W) cameras. Some of these photographs (Fig 1) have revealed evidence of possible life either as fossil-like features or of living organisms such as the lozenge-shaped 'rice grains' (Joseph et al. 2020a, Rizzo et al. 2021), spherules (Joseph et al. 2020a, 2021), and suggestive of stromatolites (Rizzo & Cantasano 2009; Bianciardi et al. 2014, 2015, Joseph et al 2020a, Rizzo & Bianciardi 2024), lichens (Joseph et al. 2020a, Armstrong 2004, 2019a, 2019b, 2023), microbialites (Rizzo &

Bianciardi 2024), microbial mats (Joseph et al. 2020a), and biofilms (Rizzo & Bianciardi 2024) in addition to various metazoans (Joseph et al. 2020b, 2023a,b) and sponges (Armstrong 2022a).

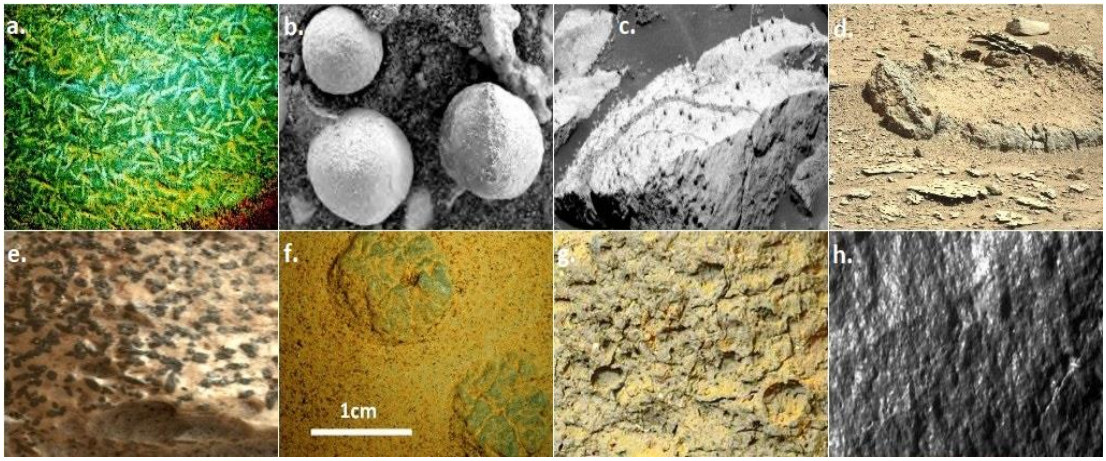

Fig 1. Examples of Martian specimens suggesting the presence of microbial life: (a) 'rice grains' (Curiosity: Sol 809), (b) spherules (Opportunity: Sol 1148), (c) stalked spherules (Opportunity: Sol 85), (d) possible 'stromatolite' (Curiosity: Sol 528), (e) possible 'lichen' 'Grange' (Curiosity: Sol 2217), (f) microbialites (Curiosity: Sol 890), (g) microbial mat (Curiosity: Sol 305), (h) possible 'biofilm' (Opportunity: Sol 4009) (NASA/JPL – Caltech)

The information which can be obtained from these photographs, however, is often limited, difficult to interpret, and highly controversial. Image analysis followed by statistical evaluation may be one method of helping to determine whether an observed feature is evidence of a biological origin or more likely the result of an abiotic process.

Image analysis enables visible features to be enhanced using brightness, contrast, sharpening, and edge detection to optimize their appearance and to establish their boundaries so that quantitative measurements can be made more objectively. A number of surface features visible on Mars have been visualized and quantified using such methods including the dense populations of spherules, photographed by Opportunity at various locations at *Meridiani Planum* (Sols 28 – 97) and which have been interpreted as deposits of hematite exposed as the result of rock erosion (Fig 1b,c) (Christensen et al. 2004, Klingelhoefer et al. 2004, Soderblom et al. 2004, Squyres et al., 2004, Aubrey et al. 2007). In addition, populations of lozenge-shaped objects resembling 'rice grains', embedded in the mudstone and siltstone at the base of Mount Sharpe (McBride 2015), were detected by Curiosity in Gale crater (Sol 809, 880) and interpreted as pseudomorphic mineral crystals of sulphate such as gypsum or jarosite (Fig 1a) (Martin et al. 2017). A variety of geological and biological processes can also result in surface erosion of rocks including the formation of holes, depressions, pits, dimples, or cavities. These include cavities or pockets associated with crystals such as druse, geodes, and miarolitic cavities and lithophysa lined or filled with feldspar or quartz. In addition pits in sedimentary rocks may be caused by weathering, small pits resulting in 'alveolar' or 'honeycomb' weathering and large pits in 'tafoni' (Danin & Garty 1983, Rodriguez-Navarro 1998). Gas bubbles in lava can

also result in circular vesicles, as in vesicular basalt (Jones 2021), or non-circular cavities called ‘vug’. Moreover, shallow depressions or ‘dimples’ (‘regmaglypts’) can form on the surface of some meteorites as they pass through the atmosphere. Nevertheless, these structures may also be evidence of biology, e.g., the ‘rice grains’ resemble some types of terrestrial living or fossil algae (Rizzo & Castasano 2009; Bianciardi et al. 2014, 2015), the spherules, especially if stalked, resemble the fruiting bodies of certain fungi or lichens (Joseph et al. 2020a,2021, Armstrong 2021a), and the surface holes resemble those made by terrestrial rock-boring bivalves (Barrows 1917, Joseph & Armstrong 2022).

Williams et al. (2015) have listed criteria for the assessment of biotic signatures of microorganisms in rock which may also enable fossil-like features on Mars to be compared with suitable terrestrial fossils or living analogues. Nevertheless, quantitative image analysis can never prove the existence of life on Mars but may enable more objective comparisons to be made with possible terrestrial analogues. Such information may also be useful in directing further missions to the Martian surface both by suggesting changes and improvements to the protocol by which photographs are obtained and by identifying locations and features suitable for more detailed examination.

This article describes various methods for quantifying features visible in Martian photographs. First, the problem of establishing a scale measure to enable absolute measures of size is discussed. Second, methods of quantifying the abundance of a feature are described including frequency, density, coverage, and semi-quantitative scores. Third, the sampling methods by which such quantitative measures can be obtained are reviewed including plot-based and plotless sampling. Fourth, methods for determining the spatial pattern (dispersion) of a feature, i.e., whether the feature is distributed at random, regularly, or is aggregated into clusters are described (Armstrong 2022b). Fifth, methods of measuring the degree of spatial association or correlation between different features, e.g., whether patches of green ‘staining’, suggestive of green algae, on different facets of a boulder are correlated with the aspect and/or slope of the facet, are described. Sixth, analysis of the morphological characteristics of a feature is described which may enable it to be compared with possible terrestrial fossils or living organisms (Joseph et al. 2020b, Rizzo et al. 2021, Armstrong 2021a,b). These methods are illustrated with reference to the analysis of various Martian features, viz. the spherules, ‘rice grains’, a possible lichen, filamentous structures, and pitted rocks.

2. ‘Scale’ in Martian photographs

Martian photographs are usually of two types, viz. panoramic views of the landscape or more detailed views of rock, pebbles, and regolith. Many of the quantitative methods described in this article are derived from survey methods used by terrestrial ecologists and most use plots or ‘quadrats’ of suitable size and shape as basic sample units in which to estimate abundance (Cox 1990). The problem is how to establish plots of suitable size for use in measuring features on Mars and for

comparing different samples. The problem is likely to be least when examining close up photographs taken by MAHLI or S-W where it can be assumed that the camera lens is located more or less normal to the surface and therefore, that a single scale measure can be used for the whole image. Hence, an approximate scale can be fitted to some Curiosity images as follows (Rizzo et al. 2021): (1) using the 'motor count' associated with the photograph, a pixel can be converted to microns using a calibration graph, (2) the photograph can be opened using an image analysis program or 'paint' and expanded to reveal the pixels, and (3) using the calibration from pixels to μm, an appropriate scale bar can be added to the photograph. Such a bar has been fitted to an image of the 'rice grains' (Fig 2). Nevertheless, photographs may not be taken exactly normal to the surface and therefore, it may not be possible to use a single scale measure. Knowing the angle of the surface of the rock to the camera lens would be useful information in determining whether any adjustments to plot size or shape would be needed for use over different parts of a photograph.

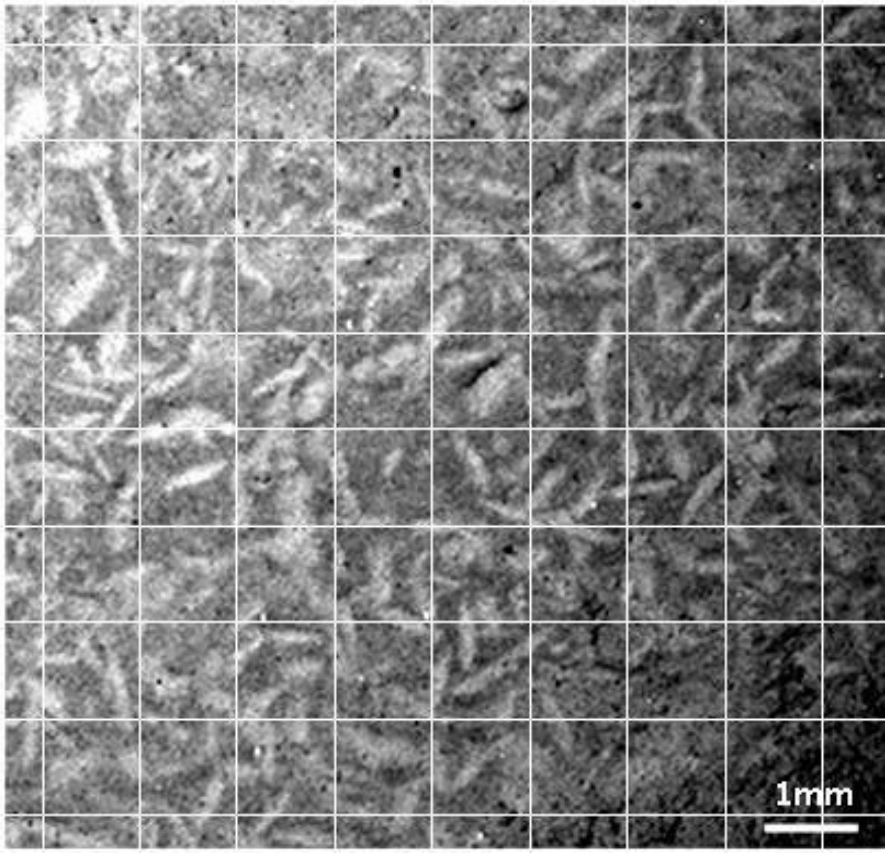

Fig 2. A population of the lozenge-shaped 'rice grains' (with sample grid and estimated scale bar) photographed by Curiosity at Gale crater (Sol 809; MH0004460030300919C00_DXXX-br2_14578)

The problem of scale is significantly greater in panoramic views of the surface and a serious problem when comparing features on boulders located at different distances from the camera and which are subject to image distortion (Fig 3). In addition, different facets of a boulder occur at variable angles, making it impossible to use a standard plot size throughout the photograph. Either features equidistant from

the camera, e.g. across the foreground, should be analyzed or plot size adjusted for distance. It may be possible in a panoramic image using data of estimated distance from the camera to a prominent feature together with focal length, angle of transect, and height of camera from the ground, to estimate the degree to which plot size would need to be adjusted as boulders become more distant. In addition, this information together with the angle of the surface relative to the frame of the photograph may provide data enabling the shape of the plot to be adjusted for both distance and angle. A more detailed discussion of the problems of estimating scale in Martian photographs is given in Armstrong & Bianciardi (2024).

Fig 3. Accumulations of ‘spherules’ among boulders on a shallow slope at *Meridiani Planum*. As a consequence of problems in fitting a scale measure to panoramic images, investigation of the spherules would need to be confined to those across the foreground of the image. Imaged by Opportunity (Sol 85; 1P135732119EFF1400P2283R1M1).

In many circumstances, it may not be possible to obtain absolute scale measures accurate enough to compare features in a series of photographs, basic measurements being made in pixels rather than on an absolute scale. Hence, if various metrics are to be derived from these measurements for comparative purposes, they will need to be ‘dimensionless’ and based on ratios of different measurements, the degree of variation among measurements using statistics such as the coefficient of variation (CV), and the degree of fit to various statistical distributions, e.g., normal, log-normal,

and Poisson distributions (Armstrong 2021a, 2021b). Examples of the use of this approach will be described at various points in the text.

3. Abundance

It may be useful to compare the abundance of a feature at different sites, among photographs taken at the same site at different times (Joseph et al. 2021), or within an individual photograph on different boulders or facets of a boulder. A number of methods are available for estimating abundance including measures of frequency, density, coverage, and semi-quantitative scores (Table 1).

Table 1. Quantitative measurements associated with different sampling methods.

	Sampling method (see section 4)		
Measurement	*Plot-based*	*Transect*	*Point-quarter*
Density (D)	$D_i = n_i/A$	$D_i = n_i/L$	$d^* = \sum d_i/\sum n$
Frequency (f)	$f_i = j_i/k$	$f_i = d_i/k$	$f_i = j_i/k$
Coverage (C)	$C_i = a_i/A$	$C_i = l_i/L$	$Ci = (a_i)(d_i)/n_i$

Abbreviations: n_i = number of individuals of feature 'i', A = Unit of area, L = total length of transect, d^* = mean point to feature index, d_i = point to feature distance, j_i = number of samples in which 'i' is present, k = total number of samples taken, a_i = total area covered by feature 'i', l_i = total area covered by lesion 'i'.

3.1 Frequency (F)

Frequency is a simple and rapid method of quantifying the abundance of a discrete feature, i.e., one that can be defined as comprising separate individuals separated from each other and distinct from the background. To determine frequency, the number of plots in a sample in which a particular feature occurs is counted such that if an object occurs in 7/10 plots, the probability of finding it in an area is 0.7 and its frequency is 70%. Frequency estimates are highly dependent on the size and shape of the plot. Hence, if several different features are investigated at the same time and vary in frequency and if the plots are too large, then it is certain that all features, common or rare, will be recorded whereas if the plots are too small, then less common features may be excluded. Frequency measurements are also sensitive to the distribution of the objects, i.e., whether they are distributed at random, regularly, or are aggregated into clusters (Armstrong 2022b). Many features in Martian photographs, e.g. the ‘rice grains’ appear to be distributed at random but terrestrial living entities, especially plants and sessile animals, often exhibit a clustered distribution (Greig-Smith 1952,1964; Kershaw 1973) and sample plots of different size may be necessary to estimate frequency.

3.2 Density (D)

To determine density, the number of individual objects is counted in sample plots and the numbers averaged and expressed per unit of area, volume, or arbitrary units if no scale measure is available. There are two problems in obtaining accurate density measurements. First, it may be difficult to define an appropriate area in which the density measurement is to be obtained. For example, an object may develop in relation to a specific type of rock and sampling may need to be confined to such rocks which have particular characteristics of shape, color, or texture. Second, it may be difficult to define what constitutes an individual object or feature. Hence, although the spherules or 'rice grains' are relatively distinct, a more diffuse feature, e.g., irregular patches on rocks, may be more difficult to define. In some circumstances, it may be impossible to establish an 'individual' necessitating the use of an alternative measure such as 'coverage'

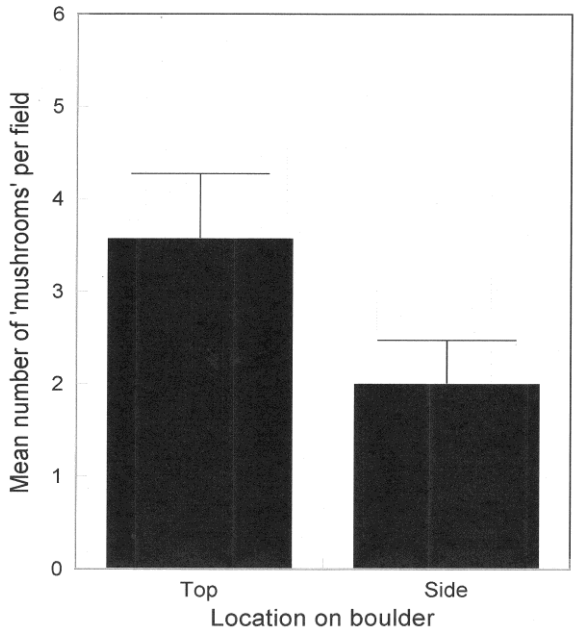

Fig 4. Mean density of spherules (Opportunity Sol 85) on the upper surfaces of boulders compared with their steeper sides (Comparison of mean numbers: Paired 't' = 5.21, $P < 0.001$)

As an example, the density of the spherules was compared on the tops and sides of a sample of 14 boulders located in the foreground of images at various sols (Opportunity, Sol 28 - 97). Boulders were restricted to the foreground to eliminate as far as possible the effect of image distortion on plot size. On each boulder, a square plot of standard size was placed at a random location on the flatter upper surface and on the adjacent steeper side and the number of spherules counted. The mean number of spherules was significantly greater on the tops compared with the sides of the boulders (Fig 4) (Paired t-test, 't' = 5.21, $P < 0.001$). Hence, if these structures are concretions gradually being exposed as a result of erosion of softer rock, it will be

necessary to explain how the stalked spherules were formed on both horizontal and vertical surfaces. If the spherules are evidence of biological activity, perhaps representing fungal or lichen fruiting bodies (Joseph et al. 2021, Armstrong 2021c) or concretions involving microorganisms, then their formation and/or survival appears to be greater on flatter surfaces. This study has two limitations. First, the data were compiled from different photographs and there is no guarantee that the camera was positioned at the same distance from the foreground boulders in each image. This is a less serious statistical problem as a comparison of the top with a side form a series of pairs of independent observations made from different boulders, and this sample of pairs can be tested by a paired sample 't' test. Nevertheless, the increased variance which would arise from the likely differences in plot sizes would reduce statistical power thus decreasing the probability of detecting, if present, a significant difference between the surfaces. Second, the shape of the plots was not adjusted for the flatter upper surfaces which may have overestimated their density.

3.3 Coverage (C)

Coverage is more closely related to the 'amount' of a feature present in a photograph and may be an appropriate measure if the objects are less circumscribed. Image analysis systems frequently provide estimates of this type of measurement by measuring 'coverage' which is the proportion of the area that is occupied by a feature in relation to the total area it could occupy. Coverage values can also be obtained by placing a grid of squares over an area containing the feature of interest (Fig 2) and counting the number of times the points of intersection of the grid 'contact' the feature under study. The number of contacts can then be expressed as a percentage of the total.

3.4 Semi-quantitative scores

A rapid method of describing the abundance of a feature is to assign a subjective abundance score. For example, a feature could be scored on a four-point scale, viz., none (0), sparse (1), moderate (2), or frequent (3). Such a scale could be used for large-scale studies employing many distinct features and photographs in which it may not be feasible to establish a consistent plot size or obtain more accurate density measurements. The limitations of semi-quantitative scores are the large unconscious error of judgment and the consequent high between-observer variability of the scores, the latter requiring independent assessment of the same feature by different observers.

4. Sampling methods

A number of sampling methods can be employed to obtain quantitative estimates of abundance from a photograph. The most commonly used are plot or quadrat-based sampling, transect sampling, and point-quarter sampling (Fig 5).

4.1 Plot-based sampling

Plot-based sampling (Fig 5a) is a commonly used procedure in ecology (Greig-Smith 1952, 1964, Kershaw 1973) and has also been used in neuropathological studies of brain histology (Armstrong 2003). The plots may be rectangular, square, or circular in shape, although the rectangular plot is regarded as the most efficient method of sampling a two-dimensional surface (Brower et al. 1990). Sample position may be determined by a grid superimposed over the photograph (Fig 5b) or other systematic method or by a standard random procedure to minimize bias. Either the analysis should be restricted to features at approximately the same distance from the camera or plot size will need to be adjusted for distance and angle. In addition, it is difficult to compare images of the same feature taken at different time periods as MAHLI and S-W are mounted on the ends of extendible arms and therefore may not be deployed at exactly the same distance from the object on each occasion (Joseph et al. 2021). Moreover, the camera may have been oriented obliquely to the surface being imaged so that the shape of the sample fields may also need to be adjusted, as for example, when comparing the tops and sides of boulders in Fig 4

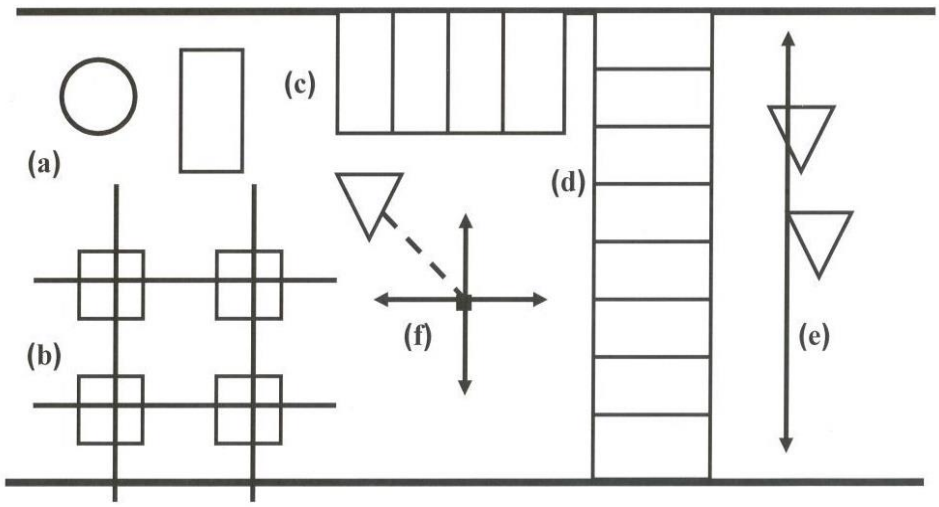

Fig 5. Sampling methods to obtain quantitative data from Martian photographs: (a) circular and rectangular plots, (b) plots arranged in a grid, (c) sampling using horizontal contiguous plots, (d) sampling using vertical contiguous plots, (e) a line transect, (f) point-quarter sampling. Inverted triangles indicate features to be sampled.

.

4.2 Transect sampling

Transect sampling is useful when there may be a systematic change in the abundance of a feature in a specific direction. A common method of sampling in terrestrial ecology is the use of contiguous, rectangular, sample fields across a region parallel to the assumed direction of a controlling variable (Armstrong 2022b). This sampling regime could be useful on Mars in studying a feature at different distances from a possible water channel, with height on the side of a boulder, or at different distances from a boulder. Two types of transect sampling can be used. First, in a 'belt-transect' (Fig 5c,d), a strip of the image is sampled in which features of interest are counted or measured. If the belt-transect is divided into contiguous plots, data for all

plots can also be used to compute density, frequency, or coverage. Second, in a line-intercept (Fig 5e), data is tabulated on the basis of features that intersect a straight line that cuts across an area to be sampled. The line-intercept method has the advantage that it is the relationship between an object and its location along a transect which is being assessed; no measurements being made, and therefore, will be less affected by image distortion.

4.3 Point-quarter sampling

Plot-based methods can be laborious and time-consuming if many photographs are studied and the results are often dependent on the size, shape, and the number of plots used (Brower et al. 1990). 'Plotless sampling' has the advantage of not demarcating sampling areas of a certain size but are sensitive to departures first, from a random distribution of individual features especially if the sample size is small (Brower et al. 1990) and second, to distance and orientation relative to the camera. The plotless sampling method of choice is the 'point-quarter method' (Fig 5f) and is regarded as superior to other plotless methods such as the nearest-neighbor method (Brower et al. 1990). To employ the point-quarter method, a number of points are established in the region of interest. These points may be randomly distributed throughout the whole photograph or randomly located along a belt-transect. Each point is considered to be the centre of four compass directions dividing the area into four quarters. In each quarter, the distance from the centre point to the nearest individual is measured; four objects to each point. Data on the mean density of the object per unit of area, frequency, and coverage can all be obtained by this method. Although plotless methods remove the problem of adjusting the size and shape of plots for distance and orientation from the camera, any linear measure would still require adjustment.

5. Spatial pattern

Measuring the spatial pattern ('dispersion') of an object, i.e., whether it is distributed randomly, regularly, or is clustered may provide a useful indication of biological origin as many terrestrial organisms cluster together rather than being distributed uniformly or at random (Greig-Smith 1952, 1964, Kershaw 1973, Armstrong 2022b). The various methods of measuring spatial pattern are summarized in Table 2.

5.1 The Poisson distribution

Methods based on the Poisson distribution are the most commonly used to measure deviation from randomness. Any type of plot sampling can be used to fit the Poisson distribution to data including randomly distributed plots, transects of contiguous plots, or grids of plots. If dispersion of individuals is random then the probability (P) that the plots contain 0, 1, 2, 3, ..., n, individuals is given by the Poisson distribution. In a Poisson distribution, the variance (V) is equal to the mean

(M) and hence, the V/M ratio is unity. The V/M ratio can therefore be used is an index of 'dispersion', uniform distributions having a V/M ratio less than unity and clustered distributions greater than unity. The significance of departure of data from a Poisson distribution can be tested using a Kolmogorov-Smirnov (KS) test and/or a chi-square (χ^2) goodness of fit test, the latter being the more sensitive (Brower et al. 1990).

Table 2. Formulae and significance tests for studying population dispersion in Martian images

Method	*Statistic*	*Significance test*	*Data*
Poisson	V/M	$t = \|V/M-1.0\|/ \sqrt{2(n-1)}$	Density
Index of aggregation (k)	$p^k(1-q)^{-k}$; p = k/k+M, q = 1 - p	none	Density
Morisita's Index (I_d)	$I_d = n (\sum X^2-N)/ N(N-1)$	$\chi^2 = (n\sum X^2/N)-N$	Density
Holgate's Index (A_1)	$A_1 = \sum (d^2/d_1^2)/ n-0.5$	$t = \|A_1\|/ (\sqrt{n}/12)$	Distance of random points to object
Hopkin's Index (A_2)	$A_2 = \sum d^2/\sum d_1^2 - 1$	$t = 2\| (A_2+1)/(A_2+2) -0.5\|\sqrt{(2n+1)}$	Point to object and object to object distances
Fourier method quantitative	-	KS test	Any data

Abbreviations: Variance (V), Individual observations (X), Mean of densities (M), Number of observations or plots (n), Total number of individuals counted on all 'n' plots (N), Distance measure (d), Student's 't' (t), Probability of an individual event (p,q)

An example of the use of the method to measure the degree of departure from randomness of the 'rice grains', imaged by Curiosity in Gale Crater (Sol 809) is shown in Fig 6. The number of such grains was counted in a sample of plots arranged at random over the photograph. No adjustment was applied to dimension or orientation of the plots as the camera lens was assumed to be located approximately normal to the surface. The KS test indicates no significant deviation from a Poisson distribution (KS = 0.12) but the more sensitive χ^2 test is more revealing (χ^2 = 17.78, P < 0.001) suggesting a degree of departure from randomness towards uniformity, which is also revealed by a V/M ratio of less than unity (V/M = 0.56). It would be possible to compare the degree of dispersion of the 'rice grains' with those of abiotic rock crystals

which resemble them, such as feldspar phenocrysts, gypsum, or jarosite to investigate further whether the 'rice grains' may have an abiotic origin.

A disadvantage of the Poisson method of determining spatial pattern is that the results are markedly affected by plot size (Armstrong 2022b). To overcome this problem, if contiguous samples or grid-sampling is used, quantitative measures in adjacent plots can be added together successively to provide the data for increasing plot sizes up to a size limited by the length of the strip or square sampled (Armstrong 2022b). V/M is plotted against the various field sizes and the resulting graph will indicate whether the clusters of objects were regularly or randomly distributed and at which scale. A peak indicates regularly distributed clusters of objects while the field size corresponding to the peak is an indication of the mean cluster size.

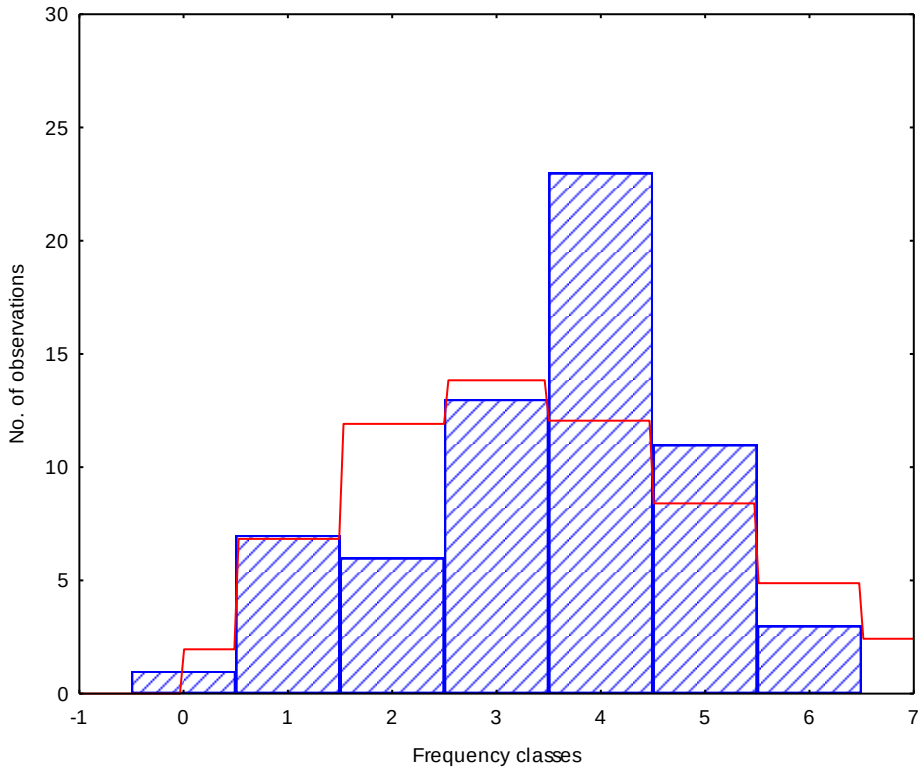

Fig 6. Spatial pattern analysis of the 'rice grains' photographed in Fig 2: Fit to the Poisson distribution: Red histogram indicates expected frequencies and blue histogram the observed frequencies (Goodness-of-fit: KS = 0.12, P > 0.05; χ^2 = 17.78, P < 0.001, V/M ratio = 0.56).

An example of this method applied to the spatial pattern of the spherules photographed by Opportunity (Sol 85) (Fig 1) is shown in Fig 7. A strip of contiguous sample fields was located across the foreground of the image across a slope running form top left to bottom right, the number of spherules being counted in each field. The spatial pattern analysis exhibits a V/M peak at 8 units, an indication that clusters of spherules are present of average dimension 8 units regularly distributed across the image. If the spherules are concretions containing hematite and originate from rock as a result of erosion, then this clustering pattern could reflect the location of unseen rock

immediately below a thin regolith together with the effects of visible patches of accumulated regolith which may have covered some individuals. Alternatively, if the spherules are evidence of biological activity, then variations in density along the transect may reflect clustering of microorganisms in the surface layers of the regolith or endolithic lichen thalli (Armstrong 2019b, 2023). Although the 'plots' in this example should strictly have followed the contours of the ground and be adjusted in shape because of image distortion, the slight distortions are unlikely to have affected the overall conclusions of the analysis.

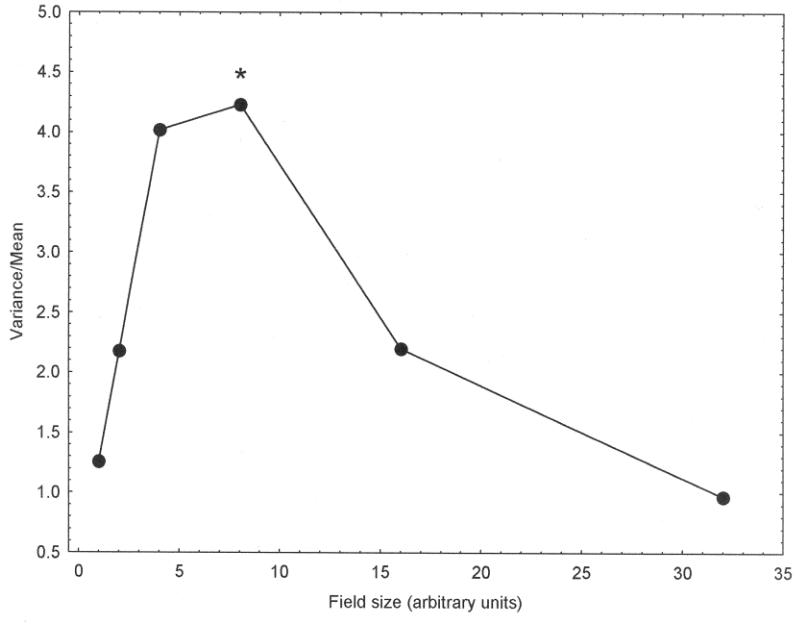

Fig 7. Pattern analysis of the spherules photographed in Fig 1 (Opportunity, Sol 85): The effect of increasing plot size (V/M = variance/mean ratio). *indicates significant V/M peak indicating the dimension of regularly distributed aggregations.

5.2 The negative binomial distribution

The negative binomial distribution can be fitted to a variety of spatial patterns in which the objects are clustered and may give a more accurate estimate of the intensity of aggregation of a feature. The negative binomial is a two-parameter distribution defined by the mean density of individuals (μ) and the binomial exponent 'k' (Table 3). The value of 'k' is generally between 0.5 and 3.0 and decreases as the degree of aggregation increases and hence, the reciprocal of 'k' can be used as an index of aggregation. The procedure for fitting the negative binomial to data is given by Cox (1990). Essentially, any sample information about the numbers of objects can be analyzed as long as the mean number of individuals per sample is low and plot size is adjusted to reflect this limitation. Data are grouped as a frequency distribution to show the number of samples (f) containing various numbers of individuals (X). The mean number of individuals per plot is then calculated and 'k' estimated by an iterative procedure (Hilton & Armstrong 2014). The expected frequencies of samples

containing various numbers of individuals can then be calculated and compared with the observed distribution to test whether the negative binomial is an adequate fit to the data.

An example of fitting the negative binomial distribution to the distribution of surface pits photographed by the rover Perseverance at Jezero Crater is shown in Fig 8. A grid of squares was overlain onto the photograph and the number of distinct pits counted in each square. From the frequency distribution of the number of pits per sample, the parameters of the negative binomial distribution can be estimated (Mean = 2.30, k = 2.40) which are then used to calculate the expected number of pits per sample. Although the sample size is small, the observed data do not deviate significantly from the negative binomial distribution (χ^2 = 2.52, P = 0.96), indicating that the pits occur in clusters similar to those associated with terrestrial rock-boring bivalves (Joseph and Armstrong 2022).

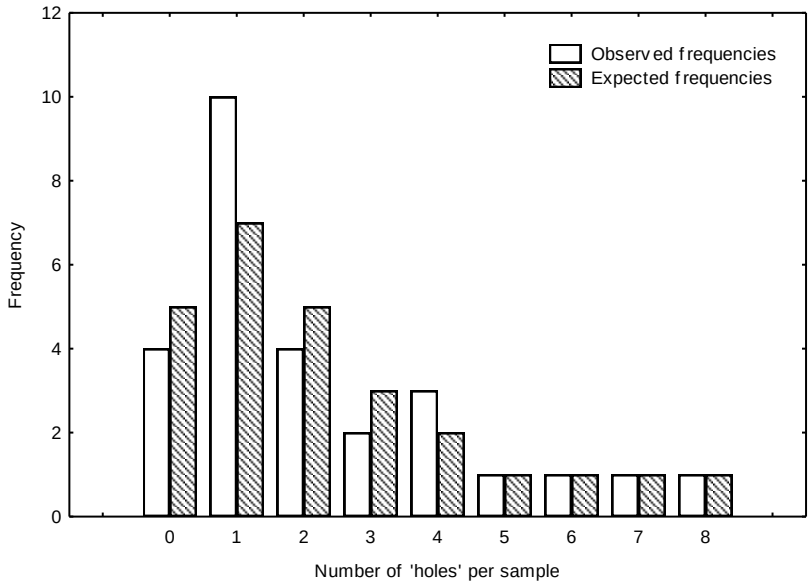

Fig 9. Fitting the negative binomial distribution to the surface ‘pitted holes’ on a rock photographed at Jezero crater by the Perseverance rover. Fit to the negative binomial distribution (χ^2 = 2.52, P = 0.96)

4.3 Morisita's index of dispersion

Morisita's index of dispersion (Morisita 1959) has the additional advantage that if an object was originally clustered, the index is unaltered if objects have disappeared at random over time from the original clusters. This may be especially relevant on Mars as any object on the surface of the boulders, such as the spherules, other than those protected on the steeper sides or in deep crevices, will be vulnerable to the scouring effects of wind. Some of the stalked spherules observed in Martian images are bent over and some have broken off the rock (Joseph et al. 2021). In addition, the spherules also appear denser when associated with the regolith between boulders than on the exposed surfaces of boulders, which may reflect a less vulnerable location. Morisita's index of clustering (I_d) (Table 3) is unity for a random distribution, zero for

a perfectly uniform distribution, and equal to 'n' when individuals are maximally clustered. The significance of I_d can be tested by a χ^2 test (Table 3).

4.4 Plotless methods of determining population dispersion

Since the degree of dispersion of an object is dependent on plot size, methods have been developed for analyzing population dispersion without the need for plots. An additional advantage is that it is easier to adjust 'length' data for distance and camera angle compared with 2D plots. In Holgate's method (Holgate 1965), a number of randomly selected points ('n' at least 50) are marked on the photograph. From each point, the distance to the nearest object of interest (d) is measured and the distance to the second nearest object (d_1). The index of aggregation (A_1) (Table 2) is zero for a random distribution, greater than zero for a contagious distribution, and less than zero for a uniform distribution.

In Hopkin's method (Hopkins 1954), a number of points are first, marked at random and the distance of each point to the nearest object measured (d). Second, a total of 'n' objects are selected at random and the distance from each to the nearest object measured (d_1). The index of aggregation A_2 (Table 2) is zero for a random distribution, greater than zero for a contagious distribution, and less than zero for a uniform distribution.

4.5 Pattern Analysis Using the Fourier Method

There are several disadvantages of the Poisson distribution to investigate spatial pattern. First, only density data can be analyzed and not quantitative measures of abundance such as the amount of a feature or coverage. Hence, a Martian feature may consist of diffuse patches rather than discrete objects and not be amenable to analysis by the V/M method. Second, the abundance of a feature may vary linearly along a transect, or a single large cluster may dominate an area, thus making it more difficult to detect spatial pattern at smaller scales. Third, cluster size estimates can be inaccurate making it more difficult to determine the causes of the pattern. Fourth, objects such as the spherules may be present at high density, and not in discrete clusters, and may exhibit continuous fluctuations in abundance. Fifth, there may be repetitive fluctuations in density at different scales, i.e. large- and small-scale fluctuations, which are not well detected using previous methods. The advantage of Fourier (spectral) analysis is that it can take into account many of these problems (Armstrong 2022b). Hence, Fourier analysis detects the pattern of fluctuations in space or time which are broken down to reveal their constituent sine waves. The original measurements may comprise sine waves of different frequency which correspond to fluctuations repeating at different scales. This method has been applied to detect patterns in many fields including physics, mathematics, imaging, probability theory, and acoustics (Shumway 1988, Shumway & Stoffer 2000).

An example of this type of analysis applied to the spherules imaged in Fig 1 is shown in Fig 9. Single-spectrum (Fourier) analysis using STATISTICA software

(Statsoft Inc., 2300 East 14th St, Tulsa, Ok, 74104, USA) was used to analyze the data. First, variations in the density of spherules along the transect were investigated for a linear trend. If detected, a linear trend can obscure clustering at smaller scales and the data are'corrected' to remove its effects. Second, a test of whether there are statistically significant sinusoidal fluctuations present is carried out. If the fluctuations are random 'noise', then the raw periodogram values (spectral densities) follow an exponential distribution and this can be tested using the KS test. Third, a significant deviation from an exponential distribution indicates that sinusoidal patterns are present in the data and the periodogram values 'smoothed' to reduce measurement noise. Any significant peaks indicate the 'periods' of the fluctuations, i.e., the number of adjacent plots which encompass one complete full cycle (Fig 9). Two significant peaks are evident in the data suggesting the presence of two frequency components: (1) at a period of 2 units representing spherule density with cycles every two contiguous sample fields and (2) at a period of 13 units representing fluctuation of spherules on a larger scale with cycles recurring every 13 sample fields. Although not 'proof' that living organisms are involved in the formation of the spherules, this type of clustering is particularly characteristic of life and further observations and analyses will be needed to identify the cause of the repeating patterns.

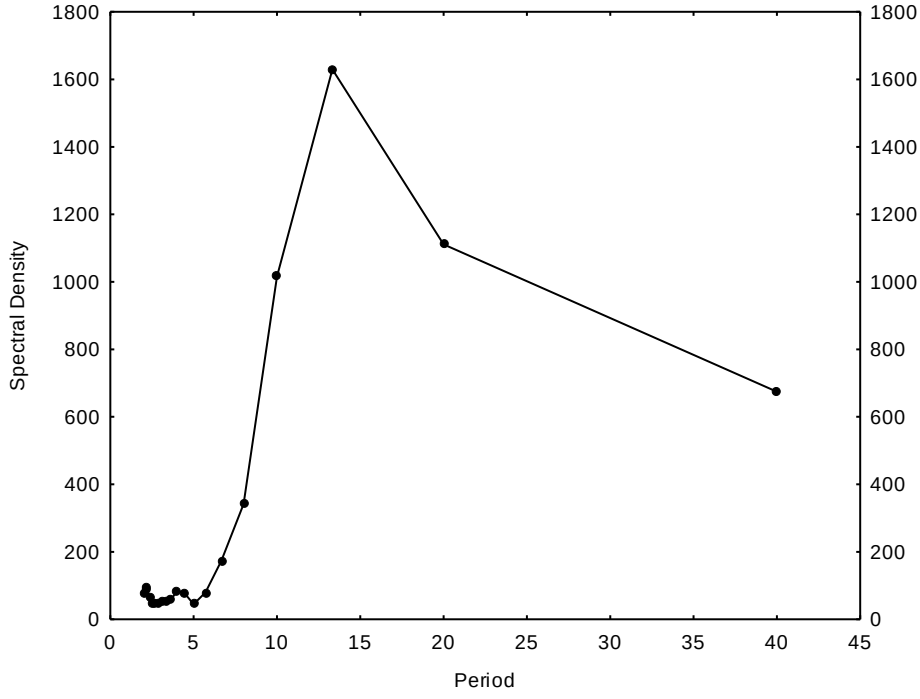

Fig 9. Pattern analysis of the spherules photographed in Fig 1 (Opportunity, Sol 85) using the Fourier method. The major peak of spectral density is located at a period of 13 units representing regular fluctuation of spherules at this scale. A smaller significant peak also occurs at a period of 2-4 units.

5. Relative orientation of objects in 2D space

A population of objects visible in a photograph may vary in 'orientation' as the development, growth, and eventual fossilization of a living organism may impose

'orientation specificity', e.g. the layered distribution of algae in stromatolites (Rizzo 2020), fungi in which fruiting bodies may be oriented to light (Joseph et al. 2021), and aquatic organisms swimming in the same direction when fossilized or oriented by wave action. In addition, features on the surface of rock or soil, such as the stalked spherules could be subjected to dust storms, distorting their shape, and resulting in changes of orientation. As an example, the orientation of each 'rice grain' in Fig 2 was measured as the angle between the horizontal edge of the sample frame and a line drawn along the maximum length of each grain. A rectangular distribution describes a variable in which each class or level of the variable is equally probable. Hence, the distribution of orientations of the 'rice grains' should fit the rectangular distribution if the profiles are random and all orientations are equally probable. The degree of fit of the orientations of the profiles in Fig 2 to a rectangular distribution is shown in Fig 10. The profiles show some evidence of departure from a rectangular distribution (KS = 0.09, $P > 0.05$; $\chi^2 = 15.39$, $P < 0.05$), profiles with orientations 120° - 160° being more frequent. The observation that this population of profiles may show a degree of orientation specificity may be an indication of a biological origin but it is also possible that mineral crystals exhibit this type of specificity.

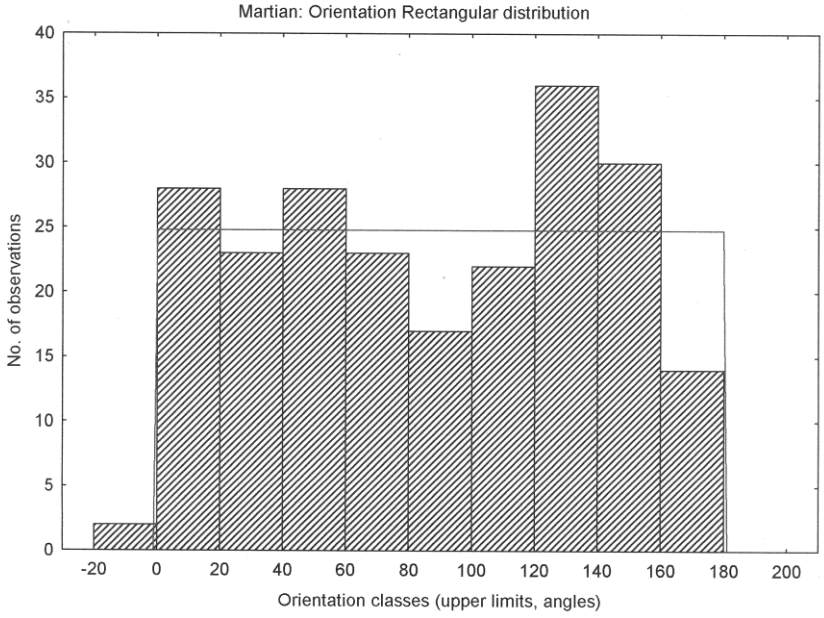

Fig 10. Relative orientation of the 'rice grains' photographed in Fig 2: Fit of the orientations of the profiles to the rectangular distribution. Horizontal straight line indicates the expected frequencies (Goodness-of-fit: KS = 0.09, $P > 0.05$; $\chi^2 = 15.39$, $P < 0.05$).

6. Spatial association

The spatial relationships between different features and between a feature and possible controlling variables may also be of interest. For example, in terrestrial environments, there may be a correlation between patches of green algae or lichen on boulders and the aspect and/or slope of the rock (Armstrong 2005a). Similarly on

Mars, there could a relationship between a feature and the topography of the ground, particularly with reference to possible damper patches underground or water channels. The existence of such correlations could be further evidence of biological origin as living organisms respond to a changing environment. In addition, it may be possible to measure the degree of association between a feature on boulders and the chemical analysis of the rock provided by ChemCam. Several methods are available for testing the degree of spatial correlation between features including methods based on contingency tables and on grids or transects of contiguous plots (Table 4).

Table 4. Formulae and significance tests for studying the association between features in Martian photographs.

Test	*Statistic*	*Significance test*	*Data*
A) Tests based on Contingency tables			
Between two features (2 x 2 Table)	C7, X^2	None, χ^2 distribution	Frequency
Between several (k) features	E (m) = NΠ (i = 1 to k) (N - n_i/N)	Normal distribution	Frequency
B) Tests using quantitative data			
Between two features	Covariance analysis $V_A + V_B = V_{AB}$ for no association	None	Any continuous variable
Between two Features	Pearson's 'r'	'r' distribution	Any continuous variable
Between several Features	'r' matrix, stepwise multiple regression	'r' and F distributions	Any continuous variable

Abbreviations: NA = not available; a, b, c, d, m, n, r, s are defined in Table 2; C_7 = Coefficient of association, χ^2 = chi-square, X^2 = chi-square corrected for continuity, V = Variance, E(M) = Expected number of empty plots, N = total frequency, k = number of different features, r = correlation coefficient.

6.1 The coefficient of association (C_7)

A simple method of testing for spatial association between two features uses qualitative (presence/absence) data arranged in a 2 x 2 contingency table. A sample of plots (N) are located at random within a region of interest and the presence or absence of the two features (A,B) recorded within each plot. From the contingency table, a 'coefficient of association' (C_7) can be calculated which varies from +1, when the maximum possible co-occurrence is present, to -1 the minimum possible co-occurrence (Hurlbert 1969). Values close to zero indicate that the frequencies of the two features are close to those that would be expected to occur by chance. The actual calculation of C_7 depends on the relationships between the numerical values in the contingency table ('a,b,c,d') and are dependent on first, whether the product of the joint presences and joint absences ('ad') is greater or less than the product of samples which contain one feature alone ('cb') and second, on the relative magnitude of 'c' and 'b' and 'a' and 'd' (Armstrong 2005b).

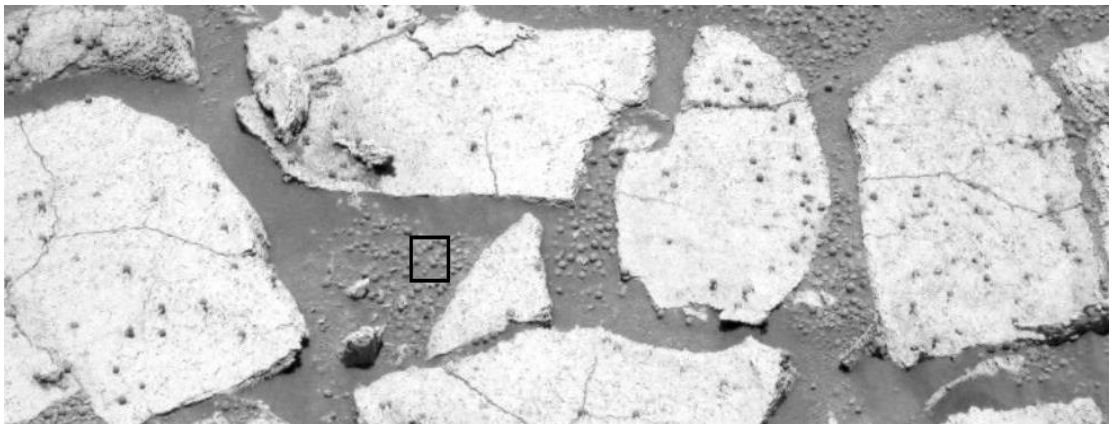

Fig 11. Measuring association between spherules and rock features using 2 x 2 contingency tables. Square sample field is shown left of centre. (Opportunity 1P135376724EFF10C0P2422L4M1)

As an example, the association between the occurrence of the spherules in an area with variously sized rocky outcrops was studied, i.e., is there an association, positive or negative, between the location of visible rocks and the occurrence of the spherules? Hence, 28 square plots, each with side dimension equal to approximately five times the mean diameter of a spherule were located at random within the region delimited in Fig 11. The presence of spherules and/or rock was recorded in each plot and the 2 x 2 table shown in Table 4. The value of C_7 was calculated to be -0.33, suggesting a weak negative association between the rocks and the spherules.

6.2 Chi-square (χ^2) in 2 x 2 contingency tables

An alternative approach to the statistic C_7 is to calculate χ^2 from the frequencies in the contingency table. χ^2 is a test of the null hypothesis that the two features are distributed independently of each other. Since the χ^2 distribution is continuous and is being used in this case to analyze discrete data, it is necessary to

make a 'correction for continuity' (Table 4) and this statistic is usually given the symbol X^2 (Pielou 1967). The value of X^2 for the data in Table 4 is 0.99 (P = 0.32) indicating no strong association between the presence of spherules and the presence/absence of the rocks. Nevertheless, Fig 11 clearly shows that there is a negative relationship between the density of the spherules and the rock outcrops which reveals the limitation of using qualitative (presence/absence) data alone.

Table 4. Degree of association between the presence of spherules and rocks at *Meridiani Planum* using 2 x 2 contingency tables (N = Row and column totals, GT = Grand total).

		Spherules		
		+	-	N
Rocks	+	a = 11	b = 11	22
	-	c = 5	d = 1	6
	N	16	12	GT = 28

$C_7 = (ad – bc)/ (a + b)(a + c) = -0.33$; $X^2 = 0.99$ (P = 0.32)

6.3 Association between many features

It may be necessary to explore the joint occurrences of more than two features of interest, e.g., whether different features visible on boulders occur together more often than expected by chance. With more than two features, the contingency tables become quite complex, but it is still possible to determine whether the features as a whole are positively associated (Table 3). A group of 'k' features are likely to be positively associated as a whole if an unexpectedly large number of plots contain representatives of all of them. Hence, it is possible to test the difference between the observed and expected frequencies for the class defined by the joint occurrences of all the features (Pielou 1967). Similarly, it would be possible to test the number of plots containing no individuals of any of the features or 'empty' plots (M).

6.4 Association based on plots

To investigate whether the density of a feature is associated with a specific variable, a series of plots can be located at different locations reflecting variations in the variable of interest. Hence, whether the density of spherules (Opportunity, Sol 85) is related to the slope angle of the rock could be studied. The data (Fig 12) collected from several boulders in the foreground of photographs show a linear decline in the number of spherules with increasing slope (Pearson's 'r' = -0.52, P < 0.01) suggesting slope of the rock may influence their formation, development, or survival.

If the sample fields are arranged in a grid or transect of contiguous plots, it is possible to study the effect of plot size and distance on the nature of the association between two features and to establish the scale at which the association is most evident. For example, a significant association between features in small plots would suggest a close relationship between them. By contrast, if association was present in

the larger plot sizes and absent in small plots, then it could be fortuitous, resulting from the abundance and widespread distribution of the two features. This aspect of spatial association can be studied either by an analysis of covariance or by the use of Pearson's correlation coefficient ('r'). In either case, a quantitative measure such as density or coverage is obtained for two features in a series of plots arranged contiguously. Quantitative measurements in adjacent fields are added together successively to provide data for larger plot sizes, e.g., two unit blocks, four unit blocks etc., up to a size limited by the length of the transect. Analysis of covariance (ANCOVA) or Pearson's 'r' can be used to determine association at each field size and the latter method has the advantage that tests of significance can also be made. If several features are studied quantitatively, then association can be studied using a correlation analysis and by stepwise multiple regression.

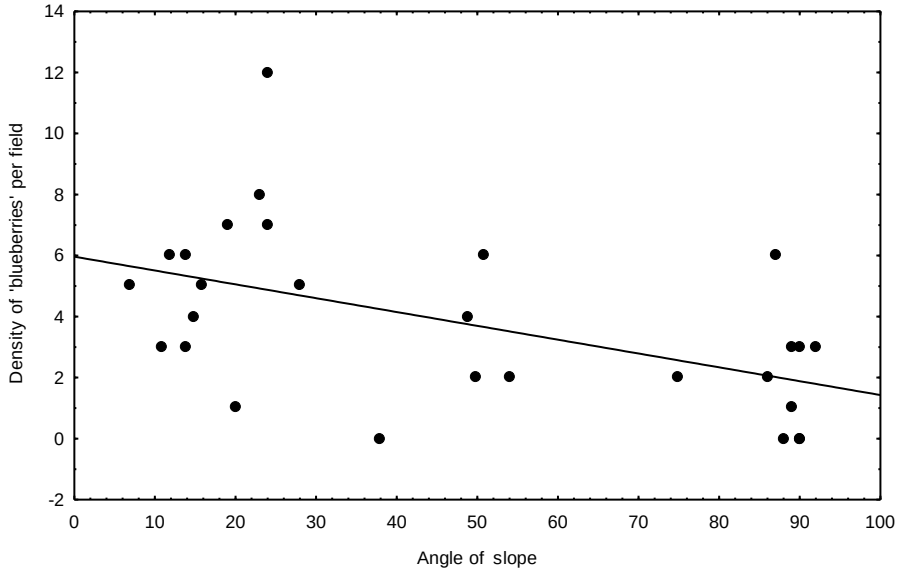

Fig 12. Change in density of the spherules photographed in Fig 3 (Opportunity, Sol 85) with slope angle of the rock (Pearson's r = -0.52, P < 0.01)

An example of the effect of field size on correlation between the density of spherules and the relative amount of regolith accumulating in a plot is shown in Fig 13. A strong negative correlation is present when measured at the first three field sizes (1,2,4) but correlations are not significant at the largest field sizes (8,16). This effect is attributable to: (1) the diminishing sample size as plots are combined to provide the larger field sizes and (2) larger plots are more likely to contain both spherules and heaps of regolith thus reducing the degree of negative correlation.

7. Quantitative morphological analysis and comparison with terrestrial analogues

7.1 Microorganisms with simple morphology

Quantitative measures describing the morphology of an object may help to decide whether there is evidence of biological origin (Armstrong & Bianciardi 2024).

This can be achieved by making a quantitative comparison between a Martian feature of interest and a possible terrestrial analogue. In addition, structures having a biological origin often exhibit certain characteristics more commonly than those with an abiotic origin (Williams et al. 2015). Hence, terrestrial microbes often exhibit a series of typical properties. First, there should be evidence of 'flexibility' and therefore objects should exhibit a degree of curvature or directional change along the object such as in bacterial or algal filaments (Schopf 2004, Hofmann et al. 2008). Second, many microbial filaments tend to have uniform diameters (Schopf 2004, Hofmann et al. 2008) while others have a uniform diameter along most of their length but have tapered ends giving rise to a characteristic 'fusiform' shape (Mares et al. 2006, Santelli et al. 2011). Nevertheless, such morphologies can also be exhibited by halotrichite minerals, the latter exhibiting a fusiform structure but with a non-uniform diameter along its length. Third, profiles should have a central lumen which may represent the original morphology of the nucleation filament. Fourth, multiple populations should be present together with numerous taxa as microbes often grow in complex communities (Schopf et al. 2007). Fifth, distinct cell walls or cellular 'elaboration' should be present. Sixth, objects should exhibit variable degrees of preservation from essentially 'life-like' through degraded, to markedly decomposed (Jones et al. 2001, Schopf et al. 2007, Jones 2010, Peng & Jones 2012).

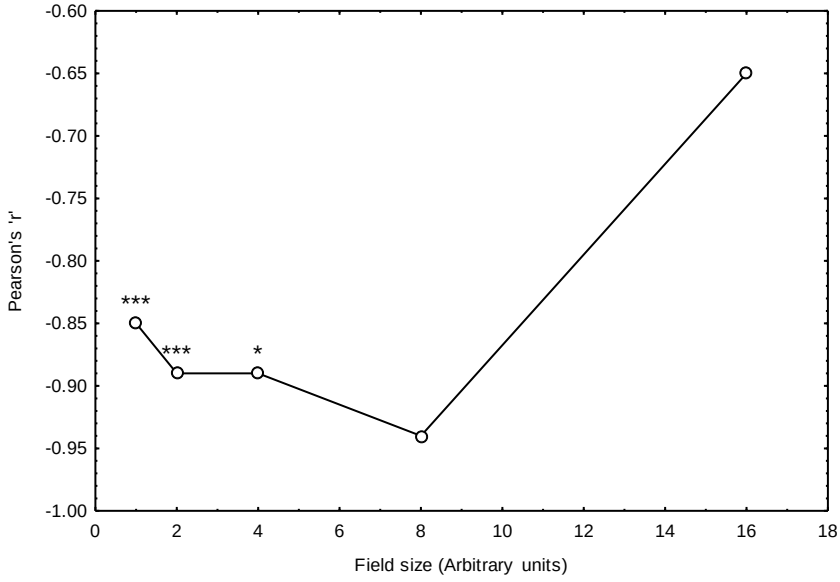

Fig 13. Investigating the influence of field size on the degree of association (Pearson's 'r') between two features (spherules and regolith) (Statistical significance ***P < 0.001; *P < 0.05)

To illustrate the method, the quantitative similarities and differences between: (1) the 'rice grains' from Gale Crater (sol 805), (2) the abiotic mineral deposit gypsum, and (3) a population of *Euglena*, a living terrestrial Eukaryote, were studied (Table 5). Both the gypsum crystals and *Euglena* superficially resemble the shape of the 'rice grains'. The only quantitative similarity among them, however, was in profile length, which for both 'rice grains' and gypsum images were fitted by a log-normal distribution. By contrast, the gypsum crystals were: (1) more uniformly distributed, (2)

more variable in length and width, (3) less likely to exhibit orientation specificity, (4) had a length/width ratio approximately 50% of that of the 'rice grains', (5) were less frequently fusiform shaped rather than rectangular, spherical, elliptical, rhomboidal, geometric, or irregular, and (5) if fusiform, were rarely curved compared with the 'rice grains'. By contrast, there were greater similarities between the 'rice grains' and the morphology of *Euglena* in (1) length/width ratio, (2) variability of lengths and widths, and (3) the percentage of profiles exhibiting a fusiform shape, and (4) in the degree of curvature. There were also some differences between the 'rice grains' and *Euglena* including a greater degree of uniformity in spatial distribution and lack of orientation specificity, the *Euglena* profiles being more similar to those of gypsum. Overall, however, it would be concluded from this analysis that the Mars 'rice grains' may have more morphological properties in common with *Euglena* than with crystals of gypsum. Nevertheless, there may be other types of sulphate-based crystals that have a quantitative signature closer to that of the rice grains such as jarosite.

Table 5. Comparison of various quantitative measures of the 'rice grains', terrestrial gypsum, and *Euglena*

Metric	*Gypsum*	*Image Euglena*	*'Rice grains'*
Number of profiles sampled (N)	169	111	411
Degree of dispersion (V/M)	0.35	0.32	0.78
Variability in profile length (CV)	74%	41%	42%
Variability in profile width (CV)	45%	16%	16%
Length/width ratio	2.3	4.42	4.1
Fit of lengths to log-normal (KS)	0.01	0.04	0.03
Fit of orientations to RD (KS)	0.07	0.09	0.09**
% Profiles fusiform shape	10%	75%	64%
% Fusiform profiles with curvature	7%	67%	57%

Abbreviations: CV = Coefficient of variation, KS = Kolmogorov-Smirnov, RD = Rectangular distribution, ** $P < 0.01$

7.2 Principal components analysis (PCA)

If two or more objects are compared based on a number of different metrics, then multivariate statistical methods can be used to display the relative similarity of one object to another. Principal components analysis ('Q-type') (PCA) is a multivariate method which enables the degree of similarity between different objects to be studied based on all of their defining features (Armstrong 2021a,b). The result of a PCA, applied to the objects under study, and which constitute the 'variables', is a scatter plot of the different objects in relation to the extracted principal components

(PC) in which the distance between pairs of objects reflects their similarity or dissimilarity. The output from such an analysis is a series of eigenvalues ('latent roots') which are proportional to the variation accounted for by each axis, the eigenvectors ('latent vectors') representing the 'loadings', i.e., the spatial co-ordinates of each object in relation to the PC. A number of PC are extracted from the data each accounting for a specific proportion of the total variance, PC1 for the greatest individual proportion of the variance and remaining PCs for diminishing amounts of the remaining variance. Normally, two or three PCs account for most of the variance within the data, the fourth and successive PCs accounting for small and diminishing amounts of the residual variation, unless considerable heterogeneity is present.

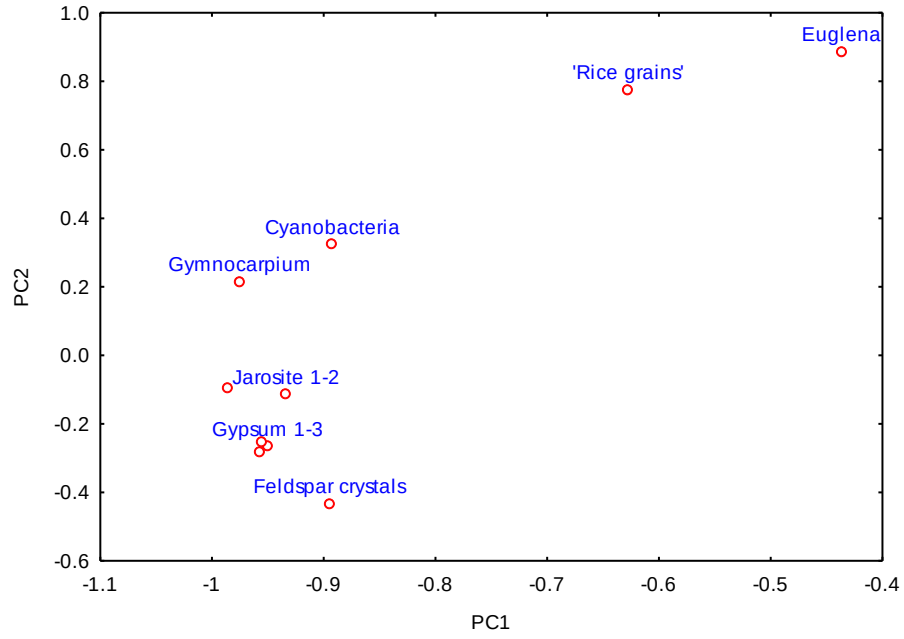

Fig 14. Principal components analysis (PCA) of Martian 'rice grains', various bacteria and algae (*Euglena*, *Gymnocarpium*, and cyanobacteria) and crystals of gypsum (3 populations), jarosite (2 populations) and feldspar. A plot of PC1 versus PC2 showing the closer affinity of the 'rice grains' to *Euglena* rather than the crystals.

An example applied to the comparison of the 'rice grains' with *Euglena* and crystals of gypsum, jarosite, and feldspar is shown in Fig 14. The spatial distribution of these variables confirms the degree of morphological similarity between the 'rice grains' and *Euglena* discussed earlier (Table 5) and their dissimilarity when compared with the rock crystals. In addition, Baucon et al. (2020) investigated quantitatively various 'stick-like' structures photographed at Rubin Ridge by Curiosity. They concluded that these structures most closely resemble the product of 'life-substrate interactions' although crystal growth and sedimentary cracking were also plausible non-biological processes. These structures were also analyzed morphologically by Joseph et al. (2020b) along with two other 'metazoan-like' fossils at Gale crater and it was concluded there was considerable morphological resemblance with known terrestrial Ediacaran fossils.

A limitation of PCA is that the analysis is strongly affected by the specific images selected and the metrics used to define them (Costello & Osborne 2005).

Hence, the analysis should be regarded as exploratory and the results therefore as preliminary as addition of further images and of additional metrics could alter the conclusions (Armstrong 2021b).

7.3 Morphometric comparisons using Deep learning (DL)

The methods described of establishing a terrestrial 'affinity' of a Martian specimen involve comparison with selected terrestrial analogues which have a similar morphology. This has been achieved either by direct comparison of morphological features or by employing a quantitative method of comparison based on various metrics and followed by an analysis using PCA (Armstrong 2021a, 2021b). Subjective assessments lack objectivity and are subject to pareidolia while PCA is sensitive to the selection of metrics used for the comparison and to the inevitably small sample sizes available (Prajapati et al. 2010, Armstrong 2021a,b). In addition, in many circumstances, a distinct recognizable object may not be present, e.g., a diffuse microbial mat or biofilm in which there may be a distinctive change in texture at the rock surface but it is not possible to establish any meaningful metrics. An alternative method is to use 'Deep learning (DL)' employing Orange Data Mining Image Analytics software to analyze the images (Armstrong and Dunne 2024a,b). This software is capable of analyzing available data largely without human intervention using a pre-trained deep convolutional neural network (Godec et al. 2019).

To carry out the analysis, one or more images of a Martian specimen are compared with a selected group of images of various terrestrial living or fossil organisms and possible non biological analogues chosen to provide a range of alternatives within a given Martian morphology. Images are analyzed using 'Orange data mining software' (version 3.35.0) (Demšar et al. 2013, Godec et al. 2019) together with various *post hoc* Image Analytics including 'hierarchical clustering' (HC) and 'multidimensional scaling' (MDS). Images are inputed as PNG files for compatibility with Orange software and then 'embedded' using 'Google Inception V3 deep convolutional neural network learning' which extracts 2048 column vectors from each image (Szegady et al. 2016). This is the software default method and although other methods are available, their relative utility in the analysis of Martian images has not yet been evaluated. The columns are 'normalized' to ensure equal weighting of all 2048 vectors. 'Distances' are then computed among the vector columns using the 'cosine metric' which is known to work well with image vectors and reflects the degree of similarity among images. The data are then subject to two further analyses: (1) hierarchical clustering (HC) (using the default 'Ward' method) and which results in a dendrogram obtained from the calculated distances and essentially 'classifies' the relationships between the various images and (2) multiple dimensional scaling (MDS) which displays the relationships between the images spatially in 2D or 3D, the distances between images reflecting their degree of similarity, a method essentially analogous to PCA.

As an example, the methodology was applied to a 'lichen-like' specimen photographed on Mars by the Opportunity rover 'Mars Hand Lens Imager' (MAHLI)

on sol 962 (Fig 15). This specimen shows the following 'lichen' features: (1) a wrinkled 'crust' suggestive of a crustose 'thallus', one of the commonest of terrestrial lichen growth forms (Armstrong 2019a,b), (2) the crust is apparently divided up into segments, a typical feature of many terrestrial lichens, and (3) a small number of circular structures with dark centers and a lighter, distinct margin similar to many terrestrial lichens which have 'lecanorine-type' apothecia. Equally, however, the 'thallus' could be a superficial mineral deposit and the 'apothecia' a type of mineral inclusion, perhaps the remains of the stalks of 'spherules' which are abundant at many of the sites visited by Opportunity (Armstrong 2021a).

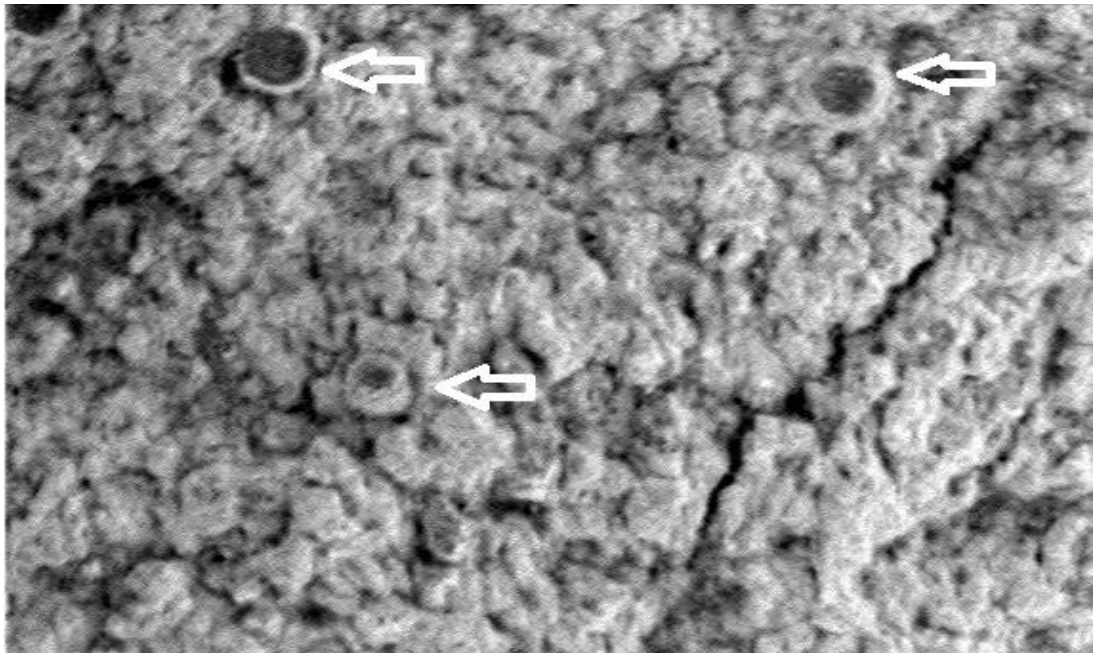

Fig 15. A Martian lichen? Opportunity Sol 962/1M2135861EFF76P0P2957M2M1 (MAHLI): Lichen-like structure showing a wrinkled surface crust and scattered circular features (approximately 1 – 2 mm in diameter) resembling 'lecanorine-type apothecia' (arrows) (Image courtesy: NASA/JPL - Caltech)

The results of the HC analysis are shown in Fig 16. Specimens which resemble each other are joined towards the right of the dendrogram, the analysis proceeding to join more and more dissimilar specimens sequentially from right to left until all are joined at the extreme left. Hence, the further to the left joining occurs the less likely it is to represent a credible match. The only terrestrial lichen which shows some linkage to the Martian specimen is the species *Chrysothrix flavovirens* Tønsberg, which is joined at a level of approximately 0.34 and therefore, not indicative of a close match. No further lichens are joined to the Martian specimen until a group of 15 species which are joined at a level of about 0.62.

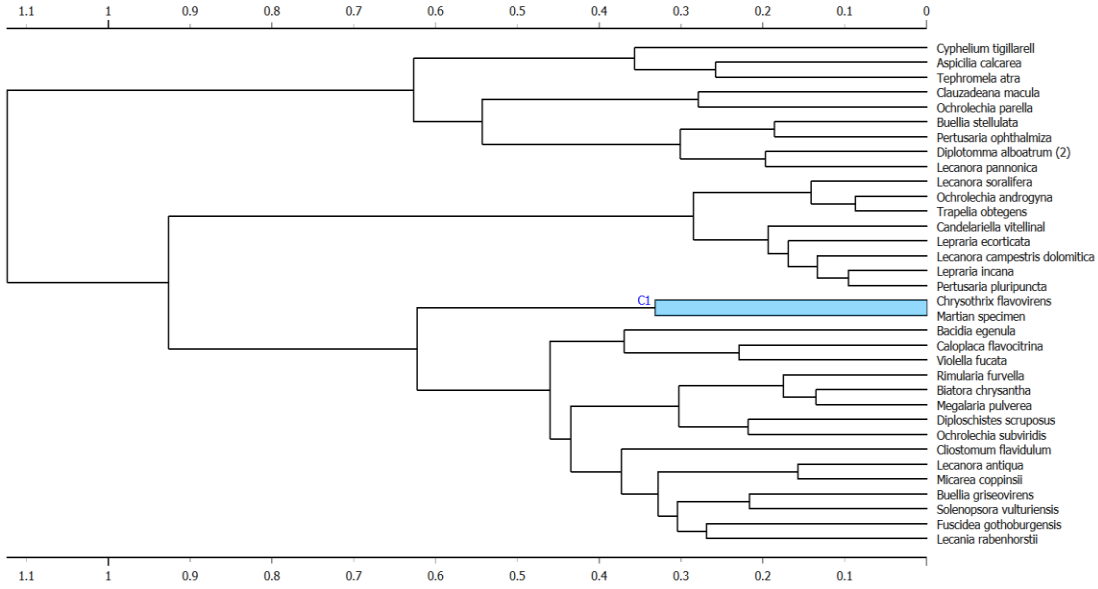

Fig 16. Hierarchical clustering (HC) dendrogram of the Martian specimen and 33 terrestrial lichens of similar morphology listed at the right using Orange Data Mining software. The terrestrial lichens with the closest linkage to the Martian specimen are highlighted in blue.

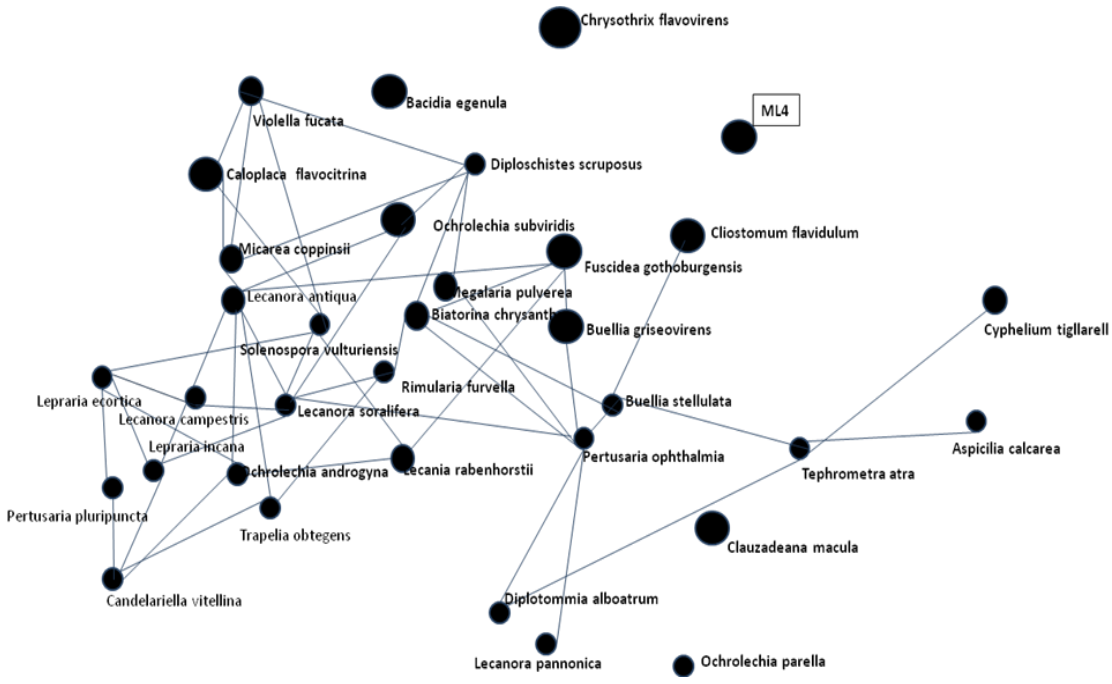

Fig 17. Multiple dimensional scaling (MDS) of the images using Orange Data Mining Image Analytics software. ML4 indicates the position of the Mars lichen-like specimen. Lines represent matches between images exhibiting similar characteristics. Larger symbol sizes indicate less confidence in each image's position in the 2D approximation of the multi-dimensional model.

The results of the MDS are shown in Fig 17. Although as anticipated there are many complex matches among the 33 species of terrestrial lichens, none are directly linked to the Martian specimen. In addition, although the species *C. flavovirens,* which the HC identified as having the closest linkage, is located relatively close to the Martian specimen, no significant match was identified by the MDS. *Chrysothrix flavovirens* is also represented by a large symbol which indicates uncertainly regarding its actual position. Hence, none of the terrestrial lichens included in the analysis provides a convincing match for the Martian specimen suggesting that it may be of abiotic origin. Nevertheless, the method offers considerable potential for the detection of possible life signs on Mars. Further examples of the use of DL to analyze Martian images are given in Armstrong & Bianciardi (2024).

7.4 Organisms with a complex morphology

Analysis of affinities using metrics or PCA have most frequently been applied to Martian specimens with a relatively simple morphology such as a single celled or calcareous algae or microbial filaments. Many plants, including more complex algae and lichens and animals such as sponges and corals (Armstrong 2022a), however, grow in an 'indeterminate' manner often resulting in a complex branched structure which makes the analysis of morphology significantly more complex (Konglerd et al. 2017). Future rover missions on Mars have the potential for revealing objects which may have these more complex morphologies. As a result, 2D and 3D imaging may be necessary to obtain quantitative characteristics related to a possible growth form which can be used to construct a 2D 'skeleton' of a branching object which can then be used to measure biologically relevant characteristics such as branch thickness, angles between branches, and spacing (Kaandorp 1999, Kruszyński et al. 2007). Software is also available for measuring properties from such a 'skeleton' (Le Bot et al. 2010, Leitner et al. 2013, Clark et al. 2013).

7.5 Fractal analysis

Fractal morphology of 'skeletonized' images can also be used to compare different features, fractal analysis software being used to evaluate their 'fractal dimension' (Bianciardi et al. 2014, Rizzo et al 2021). This method was used by Rizzo et al. (2021) to analyze the shape of the 'rice grains' at Gale Crater. First, 'rice grain' images were enlarged 10 times and opened by software such as 'Paint' to extract the specimen of interest. The extracted image was then loaded onto 'Digital Image Magnifier' (Nikolao Strikos, https://sourceforge.net/projects/digitalimagemag/) in order to apply a 'Canny edge filter' to the image using fixed Sigma, High and Low thresholds, the result being a skeletonized image. A negative of the skeletonized image was then obtained in order to evaluate the 'fractal dimension' of the image. Fractal dimension (D_0) is a measure of the space-filling properties of a structure, and is calculated by the 'box-counting' method. Hence, a series of grids are overlain over the image (5 to 100 pixels in dimension) and the frequency of boxes containing any part of the outline counted. A graph of log (the side length of the square) against the log

(number of outline-containing squares) is plotted, the slope of which represents the local fractal dimension of the image. The degree of linearity of the log-log plot is tested by Pearson's 'r'. As a result, the fractal dimension of the 'rice grains' can be compared with terrestrial analogues. The analysis suggested that the fractal dimension of the Martian 'rice grains' differs from that of the gypsum with high statistical significance ($P < 0.01$) but perfectly overlapped that of the unicellular alga *Euglena viridis* ($D = 1.570 + 0.047$ vs. $1.581 + 0.055$, mean + SD, $n = 30$ per each sample) (Rizzo et al. 2021).

Fractal analysis was also used to analyze rock surface textures in Gale crater suggestive of a complex series of branched filaments perhaps originating from a single point (Fig 18). Using Image J, the fractal dimension of this image was compared with 'skeletonized' images (Fig 19) of fungal and algal filaments and with Pele's hair, i.e., abiotic filaments resulting from volcanic glass formation. The box plots (Fig 20) indicate that the fractal dimension of the Martian filaments most closely resembled that of the fungal filaments, there being less resemblance to the algal filaments, and with significant differences to Pele's hair. This is an interesting finding as Joseph et al. (2020) also found evidence suggestive of fungi on Mars. A more detailed description of fractal analysis with a number of illustrative examples is given in Armstrong & Bianciardi (2024).

Fig 18. A branched filament-like structure on Mars suggestive of fungal or algal filaments (Curosity: Sol 1922; MH003570020703088COO_DXXX

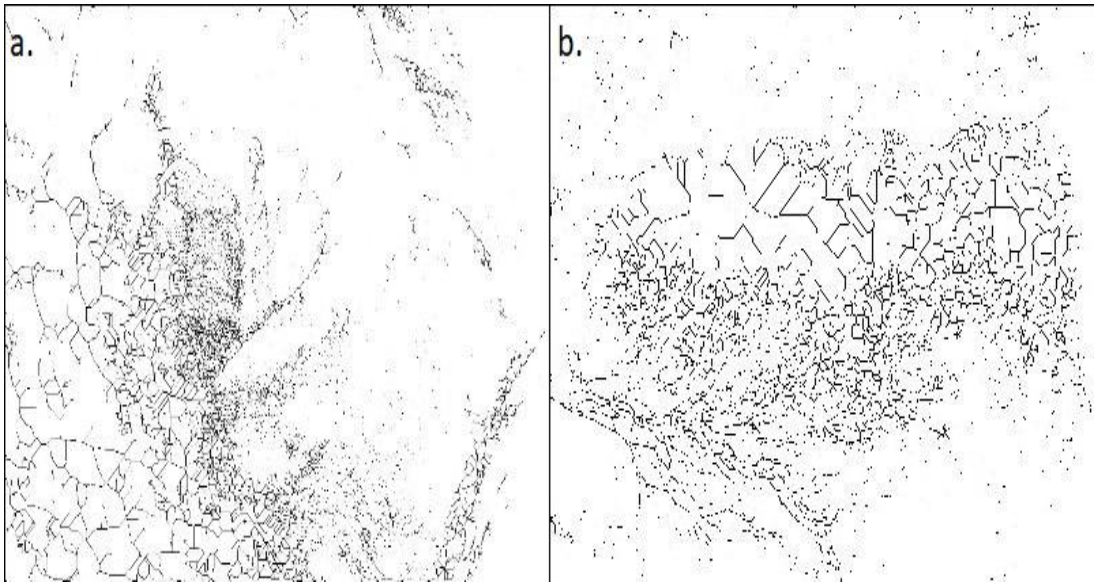

Fig 19. 'Skeletonized' images of: (a) Martian filaments (Fig 18) and (b) Fungal filaments

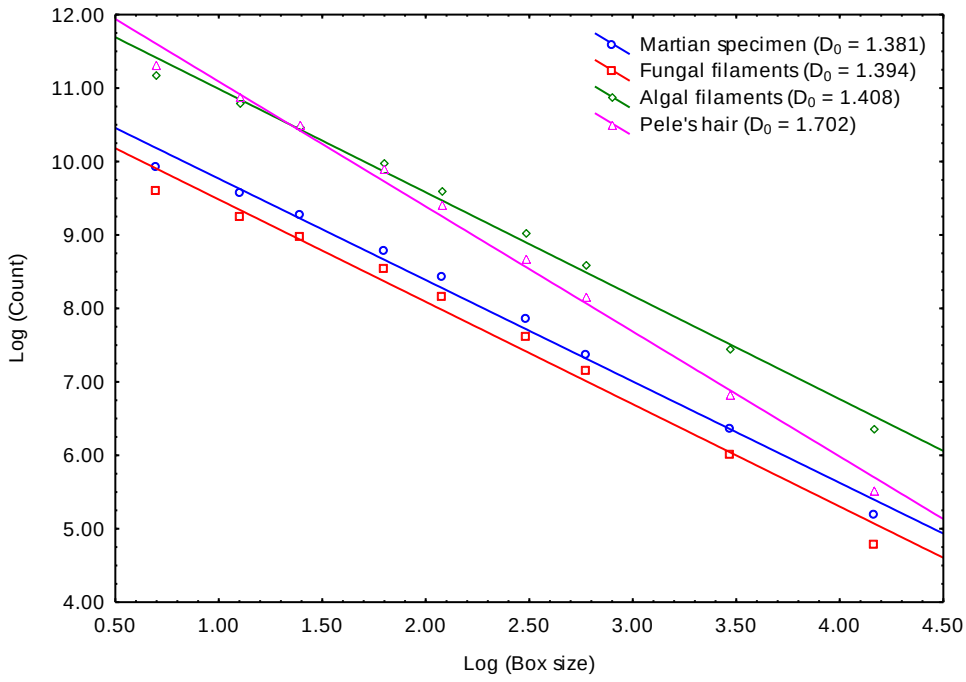

Fig 20. Box plots revealing the fractal dimension (D_0) of the Martian, fungal and algal filaments and Pele's hair

7.6 Size frequency distributions

Many terrestrial populations of organisms contain individuals at different stages of life and hence, often exhibit a characteristic age or size structure (Armstrong 2017). If there is evidence of present or past life on Mars, then it may exhibit a similar population structure (Williams et al. 2015). Many measurements made on biological

entities exhibit a normal or Gaussian distribution (Snedecor & Cochran 1980). By contrast, the distribution of the ages and sizes of organisms in a population often fits a log-normal distribution (Pollard 1977) and has been used to describe the size distributions of many plant and animal species (Hattis and Burmaster 1994, Limpert et al. 2001). This distribution is defined as that of a variable X such that $\log_e (X - Ø)$ is normally distributed. The distribution has three parameters: Ø (where $X > Ø$), the mean (μ), and the variance (σ^2). In many applications, the value of Ø can be assumed to be zero and a two-parameter model fitted to the data. Deviations from a log-normal model are tested using the KS and χ^2 goodness of fit tests.

To determine the factors influencing spherule formation at *Meridiani planum*, Eberl (2021) analyzed the 'particle size' distribution of the spheroids from data provided by Royer et al. (2006, 2008). Two main types of size frequency distribution were observed, viz. negatively skewed ('left-skewed') located west and south of Endurance crater and positively skewed ('right-skewed') north of Victoria crater (Eberl 2021). The data suggested that initial high rates of supersaturation, initiation of abundant nuclei precipitates followed by differential growth of the aggregates could account for the size frequency distributions. Many of the distributions appeared to fit either a model proposed by Lifshitz and Slyozov (1960) and Wagner (1961) ('Ostwald model of ripening') or a log-normal distribution described above.

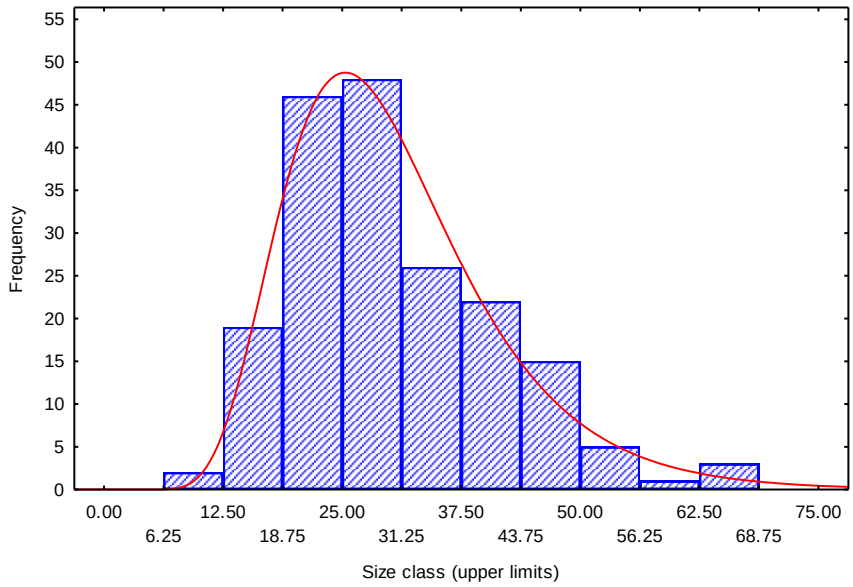

Fig 21. Size class frequency distribution of the 'rice grains' photographed in Fig 2: Fit of the lengths of the profiles to the log-normal distribution. Red curve indicates expected frequencies (Goodness-of-fit: KS = 0.04, P > 0.05; χ^2 = 3.68, P .> 0.05).

As an example, the degree of fit of the lengths of the 'rice grain' profiles (Fig 2) to a log-normal distribution is shown in Fig 21. The 'rice grains' show no significant departure from a log-normal distribution (KS = 0.04, P > 0.05; χ^2 = 3.68, P > 0.05) and therefore, exhibit a distribution similar to that of many terrestrial biological

populations, including size structures of trees and lichen thalli (Armstrong 2017). Nevertheless, a good fit to a log-normal distribution would not in itself be proof of life on Mars, as non biological structures such as rock crystals may exhibit a similar degree of fit. Quantitative studies of a variety of rock minerals and crystals are needed to test this hypothesis.

7.7 Dendrogram analysis

In some circumstances, multivariate methods of 'classification' may be useful in a comparative study. For example, many different types of rock with varying surface erosion patterns (holes, pits, cavities, depressions) are visible in the boulder field at the Viking 2 (V2) landing site at *Utopia Planitia* (Schild & Joseph 2022). Many of these rocks have holes and cavities which resemble vesicular basalt or tafoni while others resemble those previously observed at Jezero crater and photographed by the Perseverance rover (Joseph & Armstrong 2022). To investigate the range of rock morphology at the V2 site and to determine whether their surface features could be indications of current or fossil life, a morphological analysis of the populations of holes/cavities/depressions was made on a sample of 20 rocks at the V2 site. Classification methods ('dendrogram analysis') can be used to determine how many distinct types of surface erosion pattern may be present among the rocks (Clifford & Sokal 1975).

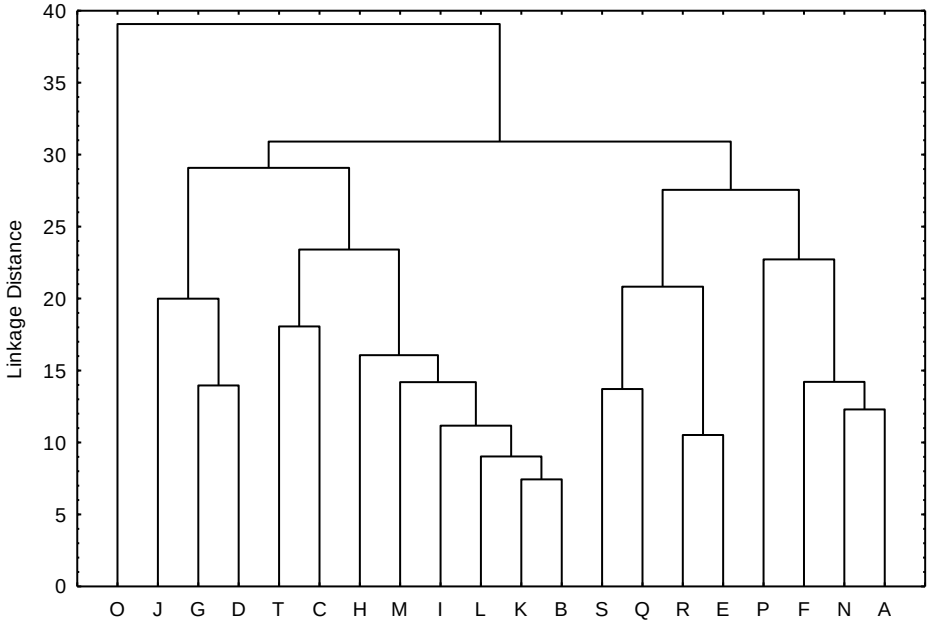

Fig 22. Classification (dendrogram analysis) of 20 populations of holes on rocks (A - T) from *Utopia Planitia*. Five groups of rocks are recognized. Note the largest cluster of rocks (Rocks T,C,F,H,I,K,L,M,B) have holes/depressions similar to those reported at Jazero crater and on terrestrial rocks associated with rock-boring bivalves. Rock 'O' is very distinct and it surface features consist of clusters of small holes.

There are several methods available for classifying data (Pielou 1967). Hence, classification methods may be 'hierarchical' or 'reticulate', 'divisive' or

'agglomerative', 'monothetic' or 'polythetic'. Moreover, several methods are available for measuring the similarity among rocks. The most commonly employed methods include nearest-neighbor, furthest-neighbor, and the un-weighted pair–group method using arithmetic averages (UPGMA) (Clifford & Sokal, 1975), the most frequently used of which is UPGMA.

To illustrate the analysis, the surface erosion patterns of a sample of 20 rocks at the V2 site were defined using a number of different metrics: (1) the degree of rock surface occupied by holes/cavities/depressions (%C), (2) the degree of radial symmetry of the hole or cavity measured as the ratio of the smallest to the greatest diameter (D_1/D_2), (3) the degree of variation in greatest diameter (D_2) over the rock surface measured as the coefficient of variation (CV-D_2), i.e. the standard deviation as a percentage of the mean, (4) the degree of variation in D_1/D_2 over the rock surface measured as CV (CV-D_1/D_2), (5) the relative spacing of the surface features measured as the ratio of the mean distance to their nearest neighbours to the mean D_2 for the population as a whole (NN/D_2), (6) the degree of fit (KS) to the log-normal distribution (LN (Hattis & Burmaster 1994, Limpert et al. 2001), (7) the variance/mean (V/M) ratio of the frequency distribution of the number of surface features in the sample fields (Armstrong 2022b), and (8) the proportion of surface features with approximately radial symmetry (i.e., $D_1/D_2 > 0.9$).

To carry out the analysis, first a distance measure *'d'* is selected which estimates the similarity of one rock to another. There are various methods of computing this distance but the most straight forward is to compute *'d'* as if the 's' variables (metrics) are dimensions making up a s-dimensional space, viz., to use 'Euclidean distance' as a measure of similarity. Second, a linkage rule is selected, the method based on UPGMA being the most commonly used. Nevertheless, the 'nearest-neighbor' method is often the default option available in various statistical packages and also offers a satisfactory method of classification.

The dendrogram obtained using UPGMA and Euclidean distance is shown in Fig 22. The process of classification is agglomerative, individual rocks being combined with those that they resemble most closely and then successively, the groups are joined as the dendrogram is ascended with ultimately, all rocks combined into a single group at the top. To determine how many groups should be retained, a useful additional plot is the 'graph of the amalgamation schedule'. As linkage distance increases, larger and larger clusters are formed but resulting in amalgamations of clusters with a greater degree of within-cluster diversity. A clear discontinuity in this graph suggests that many clusters are being amalgamated at the same linkage distance and this level can be used as an approximate 'cut-off' to determine the number of groups to retain. In the present data, this discontinuity occurs at a linkage distance of approximately 24 units indicating the presence of five types of surface erosion. Hence, Fig 22 shows: (1) one rock (O) with an erosion pattern considerably different from the rest, (2) a large group of 8 rocks (T,C,H,M,I,L,K,B) which share quantitative features with those at Jazero crater (more symmetrical holes, more variation in size, better fit to the log-normal model, and with more spacing between holes/depressions relative to their size), and (3) a remaining heterogeneous group which may be divisible into three smaller groups of

rocks (J,G,D), (S,Q,R,E,), and (P,F,N,A).

Hence, the dendrogram analysis suggests a variety of different rocks at the V2 site at *Utopia Planitia* with varying patterns of surface erosion (Fig 23). This observation is consistent with the likely repeated episodes of catastrophic flooding at the site resulting in a variety of rocks being carried into the plane from multiple sources. Of the different patterns of surface erosion identified, 8/20 rocks (Fig 23,a,b) show patterns of holes/depressions which closely resemble those at Jezero crater and on terrestrial rocks and associated with the activity of rock-boring bivalves (Joseph & Armstrong 2022). One of the rocks (Rock O) (Fig 23) is very different from the others having clusters of tiny pits and holes while the remaining 11 rocks all show considerable variation in surface features. These rocks more closely resemble alveolar weathering, tafoni, or vesicular basalt, all of which have been observed on Mars, the latter especially in Gusev crater (Rodriquez-Navarro 1998). The degree of variation among this group of rocks also suggests that a more complex combination of processes could have been involved in the development of their surface erosion patterns. More detailed analyses of a larger sample of rocks will be necessary to completely describe the variety of surface erosion patterns at *Utopia Planitia*.

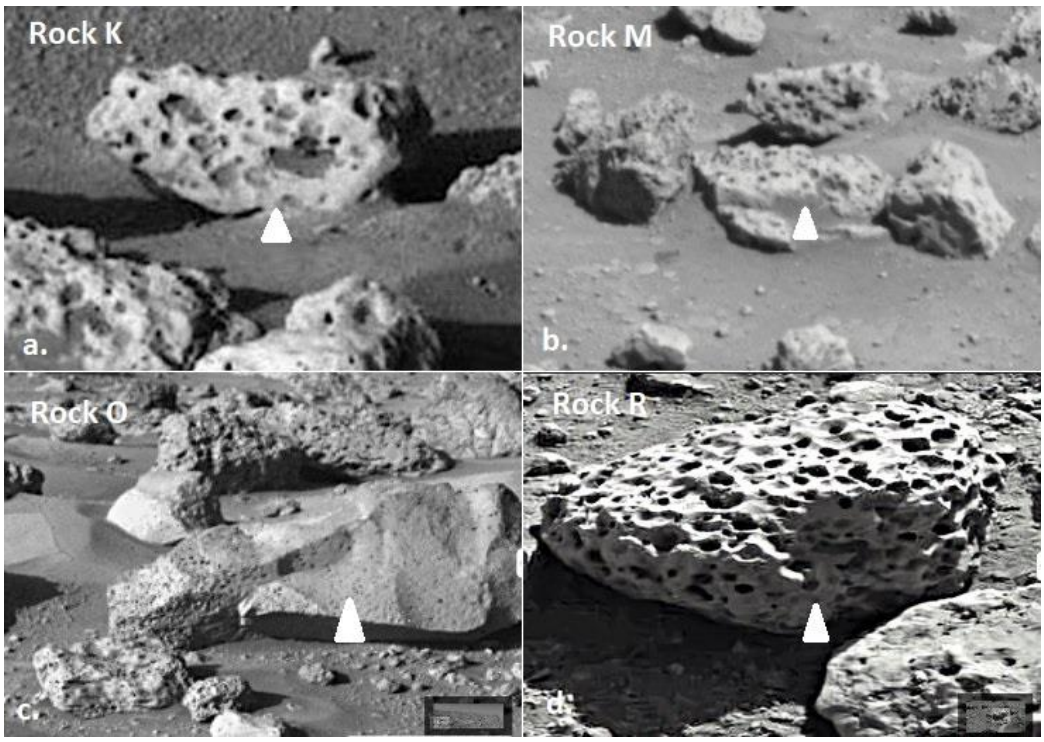

Fig 23. Examples of the different types of rocks (arrowed) and surface erosion patterns at the boulder field of the Viking 2 site at *Utopia Planitia*. Rock K resembles similar rocks photographed by Perseverance rover at Jezero Crater which may be associated with the activities of rock-boring bivalves, rocks M,R are more similar to examples of vesicular basalt or tafoni, and rock O is quite distinct with clusters of small pits.

8. Discussion and conclusions

Quantitative image analysis has been useful in many scientific disciplines including taxonomy, ecology, paleoecology, and histopathology. Hence, image analysis combined with the application of appropriate sampling strategies, quantitative measures of abundance, and data analysis methods may also be useful in astrobiology and specifically in the study of surface features visible in Martian photographs. This article reviews many of the statistical techniques which may be potentially helpful in such situations. Such an analysis in itself cannot prove the presence of life on Mars as "Extraordinary claims require extraordinary proof" (Sagan 1998). Nevertheless, it can contribute to the debate regarding life on Mars by enabling a greater objectivity to be applied to the interpretation of the numerous interesting, enigmatic, and therefore, controversial features observed in Martian photographs. Some notable examples of the use of these techniques in evaluating life signs on Mars are those of Joseph et al. (2020b,2021,2022), Rizzo et al. (2021), and Armstrong (2021a,b).

8.1 Limitations of the methods

The problem of establishing a suitable scale measure is a major problem limiting the application of quantitative survey methods to Martian photographs. These problems will affect to some extent to all studies and measurements, but are most acute when applied to panoramic photographs of the landscape in which the intention is to use plots to sample features such as boulders whose facets vary in distance and angle to the camera. The problem is likely to be least in photographs provided by MAHLI or S-W if it can be assumed that the camera lens was orientated normal to the surface. In some photographs taken by Curiosity, an approximate scale measure can be estimated using the 'motor count' and is useful in providing an indication of scale, but is still not accurate enough for comparative, quantitative analyses. In all other circumstances, in which plot sampling is envisaged, some adjustment to the size and shape of the plots may be necessary to account for image distortion. Hence, further research into suitable methods of adjustment is required to be able to fully utilize the quantitative information present in Martian photographs. One method which could be explored is to assume that a common feature, e.g. the spherules, have approximately the same mean size at all locations and adjust the size of the sample field to reflect the actual 'measured' spherule size.

A major problem of quantitative studies of Martian features is small sample sizes. Hence, although, the spherules, rice grains, and pitted rocks are locally abundant and large samples of them can be studied, many other features such as fossil-like forms are rare. Hence, in a quantitative study of 'tube worm-like' features (Armstrong 2021b), sample sizes were N = 5 and 8 for the two morphological types of 'tube worm' considered and in the study of Joseph et al. (2020b), sample sizes were N = 9, 6, and 3 for forms resembling *Namacalathus*, *Kimberella*, and Priapulids respectively. Small sample sizes result in low statistical 'power' such that small but real differences between Martian and terrestrial specimens may not be detected; a statistical Type 2 error. As discussed earlier, this problem is particularly significant when applying

exploratory multivariate methods such as PCA or dendrogram analysis, the results of which should be regarded as provisional.

A quantitative measurement needs to be relevant to the objectives of the study. Hence, frequency measurements or semi-quantitative scores often provide a quick and easy method of indicating the relative abundance of an object but lack precision and the former are highly dependent on the size and shape of the plots. They are useful in preliminary surveys of features of interest and may provide sufficiently accurate data for a more large-scale comparative study of many photographs. Density, by contrast, provides the most reliable measure of abundance, and is essential for studying dispersion and correlation with physical features, but is time consuming to obtain for large numbers of photographs. In some circumstances, individual objects cannot be identified and coverage may be a more appropriate measure than density. Semi-quantitative scores are also likely to be subject to large unconscious errors of judgment and high between-observer variability. As a consequence of the problems in obtaining scale measures accurate enough for all images, basic measurements will often have to be made in pixels rather than on an absolute scale. Hence, the metrics used to define features on Mars for comparison with terrestrial analogues are more limited and will need to be based on absolute numbers, ratios of different measurements, or on the degree of variation among measurements, measures which do not depend on establishing an accurate scale measure (Armstrong 2021a,b).

A number of different methods are available for measuring the spatial distribution of an object (Armstrong 2022b). If the objective is simply to determine whether a feature is distributed at random over the whole or part of a photograph, then one of the methods based on the Poisson distribution could be used. A major disadvantage of the simpler methods is that spatial patterns are markedly affected by the size and shape of the sample plots. Moreover, objects of interest may exhibit more complex spatial patterns. In these cases, analyses based on grids or transects using the V/M ratio or Fourier spectral analysis can provide information on the different scales at which patterns are evident as well as the ‘intensity’ and ‘grain’ of a spatial pattern. An alternative strategy is to use a plotless method of sampling that involves determining the distance between an object and its nearest neighbor. A problem in applying these methods is that the object nearest to a random point cannot be taken as a ‘randomly chosen’ member of the population as this would result in a biased sample (Pielou 1967). Hence, a random individual would have to be selected from the population of objects as a whole. This would require a complete census of the population and would be a difficult task if the feature was especially numerous.

Methods of testing the degree of association between two features fall into two distinct categories, viz., those based on contingency tables in which the presence and absence of features are analyzed, and more quantitative methods which use transects or grids of contiguous plots. Methods based on contingency tables are particularly useful in preliminary studies to determine whether there is a positive or negative association between two features that should be investigated in more detail. Of the statistics that can be used on contingency tables, C_7 is influenced by the actual

frequencies of the features present (Hurlbert 1969). The χ^2 test is less sensitive to this problem and hence, should always be calculated along with C_7. The limitation of contingency table methods is that they rely on recording the joint presences and absences of features in defined sample plots. The correlation between two features, however, may be more complex. In these circumstances, quantitative data collected in contiguous plots at different distances from a feature may provide a much more accurate assessment of association. Association can be measured in this context either by ANCOVA or by Pearson's 'r'. The disadvantage of the former is that it is difficult to make a test of significance whereas in the latter, the test assumes that the data are a sample from a bivariate normal distribution. With more than two features, a correlation coefficient matrix of the variables and stepwise multiple regression may be required.

Methods of morphological analysis rely on: (1) a careful choice of a terrestrial analogue for comparative purposes, (2) selection of appropriate quantitative measures, and (3) choice of statistical methods to evaluate the results. Hence, a terrestrial analogue needs to be selected with features that appear to closely resemble those on Mars, which are credible as a possible life form, and more likely to be primitive, unicellular, or filamentous. In addition, possible abiotic analogues need to be studied in parallel such as hematite, gypsum, or jarosite which can also resemble possible biological features such as the 'rice grains' and spherules. Fractal analysis together with DL have considerable potential for matching Martian specimens to terrestrial analogues, the former especially if branching is evident, e.g. branched filaments and possible sponges, corals, and lichens while the latter could be used where there is only a diffuse change in texture and distinct features may be absent, e.g. microbial biofilms.

8.2 Future challenges

Extracting useful information from Martian photographs can be extremely difficult. Photographs from Mars can be of poor quality and features of interest may be distorted, out of focus, fragmentary, or photographed at different distances, angles, and under variable light conditions. As a consequence, much of the information that has been gleaned from such photographs has proved enigmatic, difficult to interpret, and highly controversial. The most recent photographs provided by Perseverance have a consistently higher quality than those of earlier rovers and it is probable there will be further improvements in future. A major future challenge will be to provide more data regarding the conditions under which a photograph was obtained especially in relation to camera settings, scale, location, and environmental conditions. This will enable image analysis methods to set more accurate scale measures and to obtain more consistent and credible quantitative data. Given that the active participation of humans on Mars may be some years into the future and scientific experiments planned for new rovers are of necessity limited in scope, quantitative analysis of photographs from the planet may make an important contribution to the search for evidence of life on Mars.

Williams et al. (2015) have listed various criteria for the assessment of biotic signatures of microorganisms in rock which may also enable fossil-like features on Mars to be compared with suitable terrestrial fossils or living analogues. Application of

quantitative analysis may be able to extend these features, e.g., degree of clustering, fit to a log-normal distribution, and orientation specificity may be also indications of biotic rather than abiotic processes.

Nevertheless, many of the approaches described in this article rely on the assumption that if there is life on Mars it will have adaptive features which resemble those in or can be predicted from terrestrial environments. Because of the long history of more extreme environmental conditions on Mars, organisms may have evolved further adaptive changes and therefore, may not closely resemble any life form on Earth. A good example is the endolithic lichen growth form characteristic of the most extreme environments on Earth, viz. the cold deserts of Antarctica (Armstrong 2019b, 2023). The Martian environment is likely to be even more hostile for lichens than the cold deserts with further adaptations required in advance of those on Earth. In these circumstances, the challenge will be to predict how life on Mars may have diverged from that on Earth given their different histories.

Acknowledgments

The inspiration for this article was the pioneering research of Dr. R.J. Joseph, Dr. G. Bianciardi, and Dr. V. Rizzo.

References

Armstrong, R. A. (2003). Quantifying the pathology of neurodegenerative disorders: quantitative measurements, sampling strategies and data analysis, Histopathology, 42, 521-529.

Armstrong, R.A. (2004). Could lichens grow on Mars? Microbiologist, 4, 30-33.

Armstrong, R.A. (2005a). Radial growth of *Rhizocarpon* section *Rhizocarpon* lichen thalli over six years at Snoqualmie Pass in the Cascade Range, Washington State. Arctic, Antarctic and Alpine Research, 37, 411-415.

Armstrong, R.A. (2005b). Is there a spatial correlation between senile plaques and neurofibrillary tangles in Alzheimer's disease. Folia Neuropathologica, 43, 133-138.

Armstrong, R.A. (2017). A study of fragmentation in lichen populations on rock surfaces using Kaplan-Meir estimator and Cox regression. Annales Botanici Fennici, 54, 169-178.

Armstrong, R.A. (2019a). The lichen symbiosis: Lichen 'extremophiles' and survival on Mars. Journal of Astrobiology and Space Science Reviews, 1, 378-399.

Armstrong, R.A. (2019b). Could lichens survive on Mars. Journal of Astrobiology and Space Science Reviews, 1, 235-241.

Armstrong, R.A. (2021a). Martian spherules: Statistical comparisons with terrestrial hematite ('Moqui balls') and podetia of the lichen Dibaeis baeomyces. Journal of Astrobiology, 7, 15-23.

Armstrong, R.A. (2021b). Statistical analysis of 'tube-like' structures on Mars photographed by Curiosity and Opportunity and comparisons with terrestrial analogues. Journal of Astrobiology, 10, 11-20.

Armstrong, R.A. (2021c). The potential of pioneer lichens in terraforming Mars. In: 'Transforming Mars', Ed. Beech M, Seckbach J, Gordon R; Chapter 21, 533-554.

Armstrong, R.A. (2022a). Forms resembling sponges or corals at Gale crater, Mars: Evidence of Fossilized life or Mineralogy? Journal of Astrobiology, 13, 4-12.

Armstrong, R.A. (2022b). Application of pattern analysis to astrobiology: The spatial distribution of features revealed by Martian rovers. In: Understanding Pattern Analysis. Ed. Ghonge MU, Nijalingappa P, and Obaid AJ. Nova Science.

Armstrong, R.A. (2023). 'Grange', an unusual 'crystalline/carbonate' object in Gale crater, Mars: Rock crystals or evidence of an endolithic lichen? Journal of Astrobiology, 13, 4-12.

Armstrong, R.A., Dunne, M.C.M. (2024a). Using Deep Learning, Cluster Analysis, and Multi-Dimensional Scaling offered by Orange Data Mining software to evaluate the Terrestrial Affinities of a Lichen-like Specimen on Mars. DOI: 10.13140/RG.2.2.14803.76322.

Armstrong, R.A.,Dunne, M.C.M. (2024b). A Sponge-Coral-like specimen at Gale Crater, Mars? Results from Deep Learning, Cluster Analysis, and Multi-Dimensional Scaling using Orange Data Mining Image Analytics. Journal of Astrobiology 15, 4-15.

Armstrong, R.A., Bianciardi, G. (2024). Morphometric comparison of Martian images with possible terrestrial counterparts. In: Rizzo V, Bianciardi G (Eds), Compelling Evidence of Fossils and Microbialites on Ancient Mars. Cambridge Scholars, Newcastle-upon-Tyne, UK

Aubrey, A.D., Parker, E., Chalmers, J.H., Lal, D., Bada, J.L., (2007). Ironstone concretions – analogs to Martian hematite spherules. Geoscience Research Division, Scripps Institution of Oceanography. Lunar and Planetary Science XXXVIII.

Barrows, A.L. (1917). Geologic significance of fossil rock-boring animals. Bulletin Geological Society America, 28, 965-972.

Baucon, A., De Carvalho, C.N., Felletti, F., Cabella, R. (2020). Ichnofossils, cracks or crystals? A test for biologicality of stick-like structures from Vera Rubin Ridge, Mars. Geosciences, 10, 39.

Bianciardi, G., Rizzo, V., Cantasano, N. (2014). Opportunity Rover's image analysis: microbialites on Mars? International Journal of Aeronautical and Space Sciences, 15, 419–433.

Bianciardi, G, Rizzo, V., Maria E. Farias, and Cantasano, N. (2015). Microbialites at Gusev crater, Mars. Astrobiology Outreach 3(5), http://dx.doi.org/10.4172/2332-2519.1000143

Bianciardi, G., Nicolo, T., Bianciardi, L. (2021). Evidence of Martian microalgae at the Pahrump Hills field site: A morphometric analysis. Journal of Astrobiology, 7, 70-79.

Brower, J.H., Zar, J.H., von Ende, CN. (1990). Field and Laboratory Methods for General Ecology. Wm. C. Brown, Dubuque, IA, USA.

Christensen, P.R., Wyatt, M.B., Glotch, T.D., et al. (2004). Mineralogy at Meridiani Planum from the MiniTES experiment on the Opportunity rover. Science, 306, 1733-1739.

Clark, R.T., Famoso, A.N., Zhao, K., Shaff, J.E., Craft, E.J., Bustamante, C.D., et al. (2013). High-throughput 2D root system phenotyping platform facilitates genetic analysis of root growth and development. Plant Cell Environment, 36, 454-456.

Clifford, H.T., Sokal, R.R. (1975). An Introduction to Numerical Classification, Academic Press, New York, NY.

Costello, A., Osborne, J. (2005). Exploratory factor analysis: Four recommendations for getting the most from your analysis. Practical Assessment Research Evaluation, 10, 1-9.

Cox. G.W. (1990). Laboratory Manual of General Ecology. Wm. M. Brown, Dubuque, IA, USA.

Danin, A., Garty, J. (1983). Distribution of cyanobacteria and lichens on hillsides of the Negev Highlands and their impact on biological weathering. Zeitschrift für Geomorhologie, 27, 423-444.

Demšar, J., Curk, T., Erjavec, A., Gorup, Č., Hočevar, T., Milutinovič, M., Možina, M., Polajnar, M., Toplak, M., Starič, A. and Štajdohar, M. (2013). Orange: data mining toolbox in Python. Journal of Machine Learning Research, 14, 2349-2353.

Eberl, D.D. (2021) On the formation of Martian blueberries. American Mineralogist, 107: 153-155.

Godec, P., Pančur, M., Ilenič, N., Čopar, A., Stražar, M., Erjavec, A., Pretnar, A., Demšar, J., Starič, A., Toplak, M. and Žagar, L. (2019). Democratized image analytics by visual programming through integration of deep models and small-scale machine learning. Nature communications, 10, 4551.

Greig-Smith, P. (1952). The use of random and contiguous quadrats in the study of the structure of plant communities. Annals of Botany, 16, 293-316.

Greig-Smith, P. (1964). Quantitative Plant Ecology. 2nd Ed., Butterworths, London

Hattis, D.B., Burmaster, D.E. (1994). Assessment of variability and uncertainty distributions for practical risk assessments. Risk Analysis, 14, 713-730.

Hilton, A., Armstrong, R.A. (2014). Statnote 37: The negative binomial distribution. Microbiologist, June, 37-39.

Hofmann, B.A., Farmer, J.D., von Blanckenburg, F., Fallick, A.E. (2008). Subsurface filamentous fabrics: an evaluation of origins based on morphological and geochemical criteria, with implications for exopaleontology. Astrobiology, 8, 87-117.

Holgate, P. (1965). Some new tests of randomness. Journal of Ecology, 53, 261-266.

Hopkins, B. (1954). A new method for determining the type of distribution of plant individuals. Annals of Botany, 18, 213-227.

Hurlbert, S.H. (1969). A coefficient of interspecific association. Ecology, 50, 1-9.

Jones, B. (2010). Speleothems in a wave-cut notch, Cayman Brac, British West Indies: the integrated product of subaerial precipitation, dissolution, and microbes. Sedimentary Geology, 232, 15-34.

Jones, B., Renaut, R.W., Rosen, M.R. (2001). Biologicality of gold- and silver-bearing siliceous sinters forming in hot (75C) anaerobic spring waters of Champagne Pool, Waiotapu, North Island, New Zealand. Journal of Geological Society of London, 158, 895-911.

Jones, C.E. (2021). Scoria and pumice. Dept of Geology & Planetary Science, University of Pittsburgh.

Joseph, R.G., Graham, L., Büdel, B., Jung, P., Kidron, G.J., Latif, K., Armstrong, R.A., Mansour, H.A., Ray, J.G., Ramis, G.J.P., Consorti, L., Rizzo, V., Gibson, C.H., Schild, R .(2020a). Mars: algae, lichens, fossils, minerals, microbial mats and stromatolites in Gale crater. Journal of Astrobiology and Space Science Reviews, 3, 40-111.

Joseph, R.G., Armstrong, R.A., Latif, K., Ashraf, M., Elewa, T., Gibson, C.H.,

Schild, R. (2020b). Metazoans on Mars? Statistical quantitative morphological analysis of fossil-like features in Gale crater. Journal of Cosmology, 29, 440-475.

Joseph, R.G., Armstrong, R.A., Wei, X., Gibson, C., Planchon, O., Duvall, D., Elewa, A.M.T., Duxbury, N.S., Rabb, H., Latif, K. and Schild, R.E. (2021). Fungi on Mars? Evidence of growth and behaviour from sequential images. www.researchgate.net/publication/351252619.

Joseph, R.G.; Armstrong, R.A. (2022). Mollusks on Mars? Rock-boring marine life in Jezero Crater: A comparative quantitative morphological analysis. Research Report (Researchgate).

Joseph, R.G., Rizzo, V., Gibson, C.H., del Gaudio, R., Sumanarathna, A.R., Armstrong, R.A., Ray, J.G., Elewa, A.M.T., Bianciardi, G., Duvall, D., Wickramasinghe, N.C., Schild, R. (2023a). Fossils on Mars: A 'Cambrian Explosion' and Burgess Shale in Gale crater? Journal of Astrophysics and Aerospace Technology, 11, ISSN: 2329-6542.

Joseph, R.G., Duvall, D., Gibson, C.H., del Gaudio, R., Elewa, A.M.T., Schild, R. (2023b). Arthropods on Mars? Annals of Experimental Biology (Researchgate: 368450160).

Kaadorp, J.A. (1999) Morphological analysis of growth forms of branching marine sessile organisms along environmental gradients. Marine Biology, 134, 295-306.

Kershaw K.A. (1973). Quantitative and Dynamic Plant Ecology. 2nd Ed., Edward Arnold, London.

Klingelhoefer, G., Morris, R.V., Bernhardt, B., et al. (2004). Jarosite and hematite at Meridiani Planum from Opportunity's Mössbauer spectrometer. Science, 306, 1740-1745.

Konglerd P., Reeb, C., Jansson, F., Kaandorp, J.A. (2017). Quantitative morphological analysis of 2D images of complex-shaped branching biological growth forms: the example of branching thalli of liverworts. BMC Research Notes 10, Article Number 103.

Kruszyński, K.J, Kaandorp, J.A., Liere, A. (2007). A computational method for quantifying morphological variation in scleractinian corals. Coral Reefs, 26, 831-840.

Le Bot, J., Serra, V., Fabre, B., Draye, X., Adamowicz, S., Pagès, L. (2010). DART: a software to analyse root system architecture and development from captured images. Plant Soil, 326, 261-273.

Leitner, D., Felderer, B., Vontobel, P., Schnepf, A. (2013). Recovering root system traits using image analysis – exemplified by 2-dimensional neutron radiography images of lupine. Plant Physiology, 164, 24-35.

Lifshiz, I.M., Slyozov, V.V. (1961) The kinetics of precipitation from supersaturated solid solutions. Journal Of Physical and Chemical Solids 19, 35-50.

Limpert, E., Stahel, W.A., Abbt, M. (2001). Log-normal distributions across the sciences: keys and clues. BioScience, 51, 341- 352.

Mares, D., Romagnoli, C., Andreotti, E., Forlani, G., Guccione, S., Vicentini, C.B. (2006). Emerging antifungal azoles and effects on Magnaporthe grisea. Mycological Research, 110, 686-696.

Martin, P.E., Farley, K.A., Baker, M.B., Malespin, C.A., Schwenzer, S.P., Cohen, B.A., Mahaffy, P.R., McAdam, A.C., Ming, D.W., Vasconcelos, P.M., Navarro-González, R.A., (2017). Two-Step K-Ar Experiment on Mars: Dating the

Diagenetic Formation of Jarosite from Amazonian Groundwaters. Journal of Geophysical Research: Planets, 122, 2803-2818.

McBride, M.J., Minitti, M.E., Stack, R.A., et al., (2015). Mars Hand Lens Imagery (MAHLI) observations at the Pahrumps Hills field site, Gale Crater. 46th Lunar and Planetary Science Conference, 2855-2856.

Morisita, M. (1959). Measuring the dispersion of individuals and analysis of distribution patterns. Mem. Fac. Sci. Kyushu Univ. Ser. E (Biol), 2, 215-235.

Peng, X., Jones, B. (2012). Rapid precipitation of silica (opal-A) disguises evidence of biologicality in high temperature geothermal deposits: case study from Dagunguo hot Spring, China. Sedimentary Geology, 257-260, 45-62.

Pielou, E.C. (1967). An Introduction to Mathematical Ecology, John Wiley, New York.

Pollard, J.H. (1979). Numerical and Statistical Techniques. Cambridge University Press, Cambridge.

Prajapati, B., Dunne, M., Armstrong, R.A. (2010). Sample size estimation and statistical power analysis. Optometry Today, July, 1-9.

Rizzo, V. (2020). Why should geological criteria used on Earth not be valid also for Mars? Seeking indications for stromatolites at the macro-scale in extinct Martian lakes. International Journal of Astrobiology, 19, 283-294.

Rizzo, V., Cantasano, N. (2009). Possible organosedimentary structures on Mars. International Journal of Astrobiology, 8, 267-280.

Rizzo, V., Armstrong, R.A., Hua, H., Cantasano, N., Nicolò, T., Bianciardi, G. (2021). Life on Mars: clues, evidence or proof? In: Solar Planets and Exoplanets, IntechOpen, Article 95531.DOI:http://dx.doi.org/10.5772/intechopen.95531.

Rizzo, V., Bianciardi, G. (2024). Compelling Evidence of Fossils and Microbialites on Ancient Mars. Cambridge Scholars, Newcastle-upon-Tyne, UK.

Rodriguez-Navarro, C. (1998). Evidence of honeycomb weathering on Mars. Geophysical Research Letters, 25, 3249-3252.

Royer, D., Nelson, J., Wallace, H.C. (2006) Mars spherule size disribution from panoramic images. Lunar and Planetary Science Conference (XXXVII), Abstract 1001.

Royer, D., Burt, D.M, Wholetz, K.H. (2008). The Mars spherule size distribution and the impact hypothesis. Lunar and Planetary Science Conference, 39, Abstract 1013. Sagan, C. (1998). Billions and billions: Thoughts on Life and Death at the brink of the Millenium. Ballantine, New York.

Santelli, C.M., Webb, S.M., Dohnalkova, A.C., Hansel, C.M. (2011). Diversity of Mn oxides produced by Mn(II)-oxidizing fungi. Geochim Cosmochim Acta, 75, 2762-2776.

Schild, R., Joseph, R.G. (2022). Life on Mars discovered by NASA's Viking landers: Lichens, algae, moss, microbial mats, vesicular trace fossils in Utopia Planitia and Chryse Planitia. ResearchGate Research Report.

Schopf, J.W. (2004). Earth's earliest biosphere: status of the hunt. In: The Precambrian Earth: Tempos and Events, Ed P.G. Eriksson, W. Altermann, D.W. Nelson, W.U. Mueller, and O. Catuneanu. Elsevier, New York, pp 516-539.

Schopf, J.W., Kudryavtsev, A.B., Czaja, A.D., Tripathi, A.B. (2007). Evidence of Archean life: stromatolites and microfossils. Precambrian Research, 158, 141-155.

Shumway, R. H. (1988). Applied Statistical Time Series Analysis. Englewood Cliffs, New Jersey, Prentice Hall.

Shumway, R. H., Stoffer, D. S. (2000). Time series analysis and its application. New York, Springer.

Snedecor, G.W., Cochran, W.G. (1980). Statistical Methods. 7th ed. Ames, Iowa State University Press.

Soderblom, L.A., Anderson, R.C and Arvidson, R.E. (2004). Soils of Eagle crater and Meridiani Planum at the Opportunity rover landing site. Science, 306, 1723-1726.

Squyres, S.W., Grotzinger, J.P., Arvidson, R.E., et al. (2004). In situ evidence for an ancient aqueous environment at Meridiani Planum, Mars. Science, 306, 1709-1714.

Szegedy, C., Vanhoucke, V., Ioffe, S., Shlens, J. & Wojna, Z. (2016). Rethinking the inception architecture for computer vision. In: Proceedings of the IEEE conference on computer vision and pattern recognition, 2818-2826.

Wagner, C. (1961) Theorie der altering von niederschlägen durch umlösen (Ostwald reifung). Zeitschrift fuer Electrochimie 65: 581-591.

Williams, A.J., Sumner, D.Y., Alpers, C.N., Karunatillake, S., Hofman, B. (2015) Preserved filamentous microbial biosignatures in the Brick Flat Gossan, Iron Mountain, California. Astrobiology, 15, 637-668.